Monitoring of the volcanic rock compositions during the 2012-2013 fissure eruption at Tolbachik volcano, Kamchatka

Anna O. Volynets [a,b], Benjamin R. Edwards[c], Dmitry Melnikov[a], Anton Yakushev[d], Irina Griboedova[d]

[a] *Institute of volcanology and seismology FEB RAS, Piip boulevard 9, Petropavlovsk-Kamchatsky 683006, Russian Federation. E-mail: a.volynets@gmail.com*

[b] *GZG, Abteilung Geochemie, Universität Göttingen, Goldschmidtstrasse 1, 37077 Göttingen, Germany*

[c] *Department of Earth Sciences, Dickinson College, Carlisle, PA, 17013. E-mail: edwardsb@dickinson.edu*

[d] *Institute of Geology of Ore Deposits, Petrography, Mineralogy and Geochemistry RAS, Staromonetnyi pereulok 35, Moscow 119017, Russian Federation E-mail: antemp@inbox.ru*

Abstract. Here we present results from monitoring of the composition of rocks produced during the 2012-2013 fissure eruption at Tolbachik volcano (FTE). Major and trace element concentrations in 75 samples are reported. Products of this eruption are represented by high alumina basaltic trachyandesites with higher alkalis and titanium contents than in all previously studied rocks of the Tolbachik monogenetic volcanic field. Rocks erupted during the first three days (27-30 November) from the northern (also called Menyailov) group of vents are the most silica- and alkali-rich (SiO_2 concentrations up to 55.35 wt. percent and K_2O up to 2.67 wt. percent). From December onwards, when the eruptive activity switched from the Menyailov vents to the southern (Naboko) group of vents, silica content dropped by 2 wt. percent, concentrations of MgO, FeO, TiO_2 and Mg# increased, and K_2O, Na_2O concentrations and K_2O/MgO ratio decreased. For the rest of the eruption the compositions of rocks remained constant and homogeneous; no systematic compositional differences between lava, bombs and scoria samples are evident. Trace element distributions in the rocks of the Menyailov and Naboko vent lavas are relatively uniform; Menyailov lavas have slightly higher Th, Nb, Hf, Y, and HREE concentrations than the Naboko vent lavas at more or less constant element ratios. We explain the initial change in geochemistry by tapping of a slightly cooler and fractionated (~3 % Mt and 8 % Cpx) upper part of the magma storage zone before the main storage area began to feed the eruption. Thermodynamic constraints show that apparent liquidus temperatures varied from 1142 ºC to 1151 ºC, and thermodynamic modeling shows that variations in compositions are consistent with a high degree of low pressure (100-300 MPa), nominally anhydrous fractionation of a parent melt compositionally similar to the 1975 Northern Breakthrough basalt. Geochemistry, petrological observations and modeling are in agreement with the newly erupted material being derived from remnant high-Al magma from the 1975-76 eruption with only slight amounts of cooling (less than 1 ºC per year) during the intervening 36 years.

Keywords. Kamchatka; Tolbachik volcano; monogenetic volcanism; basaltic trachyandesite; fractionation; thermodynamic modeling

Highlights

We present a set of lava compositions spanning 2012-13 Tolbachik fissure eruption

We document a major compositional change after the first three days of eruption

From the mid December until the end of eruption lava compositions remained constant

High alumina basaltic trachyandesites with high alkalis and Ti content were erupted

Petrological modeling shows that high-Al 1975-6 and new lavas are genetically related

1. Introduction.

1.1. Geological background.

Tolbachinsky Dol (TD) is the southern part of the largest zone of monogenetic volcanism in Kamchatka, which is superimposed on the Klyuchevskoy group of composite volcanoes at the northern end of the Kamchatka volcanic arc (Fig. 1). At its northern end, TD intersects the edifice of the Plosky Tolbachik stratovolcano. TD has formed by numerous eruptions of high-alumina, sub-alkaline basalt and basaltic andesite throughout the Holocene, and since 2 ka also by eruptions of high-Mg, medium-K basalt (Fedotov et al., 1983, 1984). The most recent prior activity took place here during an eruption in 1975-76 that is known as the Great Fissure Tolbachik Eruption (GFTE). The extensive research on the GFTE produced a series of papers and a monograph on the volcanology and petrology of the eruption (Fedotov et al., 1983, 1984; Fedotov et al., 1991; Volynets et al., 1978 and many others). The DRE volume of the erupted products was 1.44 km^3, and the area covered by lava flows was ~45 km^2. This event started in July 1975 with a highly explosive eruption of high-Mg basalts from the 'Northern Breakthrough' and lasted about 2 months. Then the center of activity moved to the south and the eruption continued from the 'Southern Breakthrough' by the effusion of high-alumina, sub-alkaline basalts and basaltic andesites until its end in December 1976. Volcanic rocks with compositions intermediate between the high-Mg and high-Al basalts were erupted during the short period at the end of the Northern Breakthrough and beginning of the Southern Breakthrough activity (Volynets et al., 1978). After almost 36 years of quiescence a new fissure eruption began on 27 November 2012 in the TD approximately 5 km north of the Northern Breakthrough. It lasted 9 months and was named the "IVS 50th anniversary Fissure Tolbachik eruption" (here – 2012-2013

fissure eruption of Tolbachik volcano; FTE). Geophysical observations of the Tolbachik volcano unrest in 2012 and the precursors of the eruption are described in detail in other papers of this special issue (Kugaenko et al., this issue; Senyukov et al., this issue; Belousov et al., 2015). Seismic and GPS data are consistent with a magma storage zone located under Plosky Tolbachik and rapid southward migration of magma to the eruption site several hours before the eruption began.

1.2. Chronology of the 2012-2013 eruption.

The new eruption started from a fissure that opened at 05:15 UTC on 27 November and formed the Igor Menyailov group of vents, which are located at N 55°47′9″/E 160°19′39″ at an elevation of 1900 m a.s.l. on the upper south slopes of Plosky Tolbachik stratovolcano (Fig. 1). About 18 hours later (Volynets, Melnikov, 2013; Melnikov, Volynets, this issue) a second fissure opened further down the slope that eventually formed the Sofia Naboko group of vents at N 55°46′6″/E 160°18′59″ at an elevation of 1650 m a.s.l. The Menyailov vents were active during the first three days of the eruption (27-30 November). After that the focus of the eruptive activity shifted exclusively to the Naboko vents and continued from there until the end of eruption in early September 2013. The intensity of the eruption was highest during the first two days when the average lava discharge rate was 440 m^3/sec (Dvigalo et al., 2014). During the next two weeks the rate of lava discharge decreased to ~140 m^3/sec, and from mid-December 2012 onwards it was practically constant at about 18-19 m^3/sec (Dvigalo et al., 2014). Although the eruption was mostly effusive, numerous small scoria cones up to 15 m high as well as a group of scoria cones up to 123 m high (Naboko vent area) were formed around the mouth of the fissure; their estimated volume is ~0.02 km^3. The volume of pyroclastic deposits at a distance up to 1.5 km from the fissure zone did not exceed 0.1 km^3. However, the total estimated volume of lava erupted between November 2012 and June 2013 is 0.52 km^3, which covered an area of 35.23 km^2 (Dvigalo et al., 2014). The total volume of material erupted during 2012-2013 episode is about 0.65-0.7 km^3 (Dvigalo et al., 2014).

While Volynets et al. (2013) published the first rock compositions documenting the initial period of eruption from its beginning until late January 2013, here we present first full set of data on the compositions of rocks that span the duration of the eruption. We also discuss the petrological evolution from the beginning until the end of eruption, and show that most of the variation can be explained by relatively simple fractionation processes from a parental magma similar in composition to that erupted from the Northern Breakthrough in 1975-6.

2. Sampling and analytical methods

The erupted material was sampled systematically throughout the eruption. When possible, samples were collected from the active lava channels (Fig. 2) and from fresh bombs and scoria. Therefore, all rock samples in this collection are strictly time-bounded and document the evolution of the lava composition from the beginning until the end of the eruption. Concentrations of the major and selected trace elements (V, Cr, Co, Ni, Cu, Zn, Rb, Sr, Y, Zr, Nb, Ba, Pb) were analyzed in 75 samples by X-ray fluorescence spectroscopy (XRF) using an Axios MAX vacuum sequential spectrometer (wavelength dispersive) made by PANalytical at the Institute of Geology of Ore Deposits, Petrography, Mineralogy, and Geochemistry, Russian Academy of Sciences (IGEM RAS). For determination of the major elements, glass disks were prepared by the induction melting of the annealed sample powders mixed with lithium borates at 1200 °C. For the determination of the trace elements, samples were prepared by cold pressing the dry powders with plastic filler in a tablet 32 mm in diameter. Analytical errors were 1-5 percent for the elements with concentrations >0.5 weight percent and up to 12 percent for the elements with concentrations < 0.5 weight percent. Additional trace elements were analyzed in 18 samples by inductively coupled plasma mass spectrometry (ICP-MS) at the Institute of Microelectronics, Technology, and High Purity Materials RAS (IMT RAS). Powdered samples were digested in an acid mixture following standard procedures described by Karandashev et al. (2008). The accuracy of the measurements was monitored by analyzing USGS standards BHVO-2 and AGV-2 and in-house reference materials. The accuracy for most trace elements was ~ 7 percent. Five more samples were analyzed for trace elements concentrations by ICP-MS at Geowissenschaftliches Zentrum at the Georg-August Universität, Göttingen (Abteilung Geochemie; ICPMS by: Perkin Elmer, type: DRC II). Digestion of 100 mg of rock powder (<63µm) was performed in a mixture of $HF+HClO_4+HNO_3$ in a closed teflon beaker at 180°C for 18 hours. The dissolvable residue was digested in 100 ml 2 percent HNO_3 adding 4 internal standard elements (Be, Rh, In, Re). Concentrations of about 50 elements were determined in solutions by comparison to matrix matched calibration points covering the concentration range in geological samples. Internal reproducibility is better than 2 percent, and external accuracy checked by GJA-2 (jap. andesite) is better than 10 to 20 percent. Results were drift corrected by monitoring one calibration point through the course of the run, and also corrected for the major oxide interferences (BaO, REEO, etc).

3. Results

3.1. Petrography and mineralogy.

All products of the eruption are black to dark-grey, sub-aphyric basaltic trachyandesites (Fig. 2). Although detailed analysis of the lava microstructures and mineral phase compositions is still in progress, here we report some principal observations of the petrography that are pertinent to understanding the rocks' genesis.

3.1.1.Phenocrysts

Volcanic rocks produced during the first three days of the 2012-2013 Tolbachik eruption are practically aphyric; only sporadic large phenocrysts of plagioclase are present. Starting on 1 December the mode of phenocrysts in lavas increased (up to 5-7 volume percent) and remained at this level until the end of the eruption. Plagioclase (Pl) is the dominant phenocryst phase and it is represented by two distinct populations of crystals. The 1st generation (Fig. 3A) comprises large (up to 1-1.5 cm on elongated axis) megacrysts, which in most cases are heavily corroded with abundant melt inclusions; starting from 1 December crystal lapilli (1-2 cm in diameter) were also erupted from the Naboko group of vents. The 2nd generation (Fig. 3B) comprises mainly microphenocrysts (≤500 μm), usually with euhedral boundaries and fewer melt inclusions. Compositionally crystals of the 1st and 2nd generation range from An48-84, with distribution maximums at An62 in the Menyailov vent lavas, and An70-72 and 80-82 in the Naboko vent lavas (Volynets et al., 2014a, 2015). Isolated phenocrysts typically show patchy, normal and reversed zoning, while the glomerocrysts erupted as lapilli have oscillatory and patchy zoning.

Olivine (Ol) is found mainly as microphenocrysts. A typical feature of Ol in the 2012-2013 lavas is the skeletal shape of the crystals, possibly indicating very fast growth rates (Fig. 3C, D). Swallow-tale Ol microphenocrysts (common in MORB pillow lavas but rather rare in the terrestrial eruption products) also are evidence of rapid cooling. Compositionally Ol ranges from Fo64-76, with Fo70-75 most prevalent (Volynets et al., 2014b). Lava from the Menyailov vents contains partly dissolved Ol crystals with higher Fo contents in the core (Fo~80) and lower at the rim (Fo74). The first lavas erupted from the Naboko vents contain reversely zoned Ol microphenocrysts (Fo73 in the core and Fo75-77 at the rim).

Clinopyroxene (Cpx) ranging in composition from augite to salite (Mg# 66-73) occurs in small glomerocrysts with Ol, Pl and Magnetite (Mt) (Volynets et al., 2014b, 2015). Menyailov vent lavas contain large zoned clinopyroxene phenocrysts. The average Ti/Al_{Cpx} ratio increases from 0.22 to 0.3 between the Menyailov and Naboko vent lavas respectively.

3.1.2. Groundmass

The groundmass has hyalopilitic, hyaline, pylotaxitic and intersertal textures (Fig. 4). The main groundmass-forming mineral is Pl ranging in composition from An41-65 (Volynets et al., 2014a, 2014b, 2015). Frequently two types of groundmass (for example, light-brown semi-transparent hyaline or hyalopilitic and non-transparent black hyalopilitic or pilotaxitic) are present in thin sections; where observed the contacts between the two types demarcate high- and low-porosity areas. Lavas from the initial stage of eruption (Menyailov vents and early-erupted parts of the Naboko vents) frequently show a very sharp contact between the two types of the groundmass (Fig. 4D), demarcated by a thin (less than 1 μm) belt of Mt crystals; similar "Mt-belts" encircle partly melted Fo crystals in Menyailov vent lava (see above) and occur in microscopic fissures and cracks in the groundmass of these samples. The contact separates a coarser-grained groundmass made of Pl (up to 10 x 80-100 μm size), Cpx and Mt (both about 5-10 μm across; also some bigger microphenocrysts of Mt are more frequent here) from a finer-grained groundmass formed by thin Pl lathes (1-3 x 5-10 μm) and abundant sub-μm sized Mt.

3.2. Geochemistry

Compositionally, all of the volcanic rocks produced during the 2012-13 eruption are basaltic trachyandesites. Those produced during the first three days of the eruption at the Menyailov vents have SiO_2 concentrations up to 55.35 weight percent and K_2O up to 2.67 weight percent (Fig. 5, Table 1); they are more acid and alkali-rich than any previously studied rocks from the Tolbachik zone of monogenetic cones. At the beginning of December, when the eruptive activity moved to the Naboko group of vents, SiO_2 concentrations dropped by 2 weight percent and remained at this level until the end of eruption. Concentrations of MgO, FeO and TiO_2 increased, while concentrations of K_2O and Na_2O decreased (Fig. 5, 6). The earliest erupted lavas from the Naboko vents (December 2^{nd}-7^{th}) have a composition intermediate between the Menyailov lavas and later lavas of the Naboko vents (mid December – end of the eruption) with respect to the concentrations of SiO_2, MgO, alkalis and K_2O/MgO ratio (Fig. 6). From the middle of December onwards, the composition of rocks remained homogeneous and constant. We did not observe any systematical compositional differences between lava, bombs and scoria samples.

Normalized concentrations for trace elements in 2012-2013 FTE basaltic trachyandesites demonstrate only subtle differences between samples from the Menyailov and Naboko vents (Fig. 7, Table 2). The Menyailov samples have slightly higher Th, Nb, Hf, Y, and HREE concentrations than the Naboko samples at more or less constant element ratios (Fig. 7A, B). All trace element patterns have typical arc signatures; relatively depleted in HFSE and enriched in LILE and LREE (Fig. 7A), with elevated fluid-mobile/HFSE ratios (Ba/Nb, Th/Ta, U/Nb). They

are also enriched in HREE relative to NMORB (average Yb_{sample}/Yb_{NMORB}=1.42 in the Menyailov samples and 1.38 in the Naboko samples). However, Nb, Ta, Zr, Hf, and Y concentrations are higher than in typical arc-front lavas (Fig. 7A) compared to the high-Mg basalts of the 1975-76 Tolbachik fissure eruption, which have concentrations of incompatible elements similar to those of the Kamchatka arc front volcanoes (Churikova et al., 2001), possibly reflecting variable enrichment of the source by these elements. Sr and Eu, on the contrary, form prominent minima at the PM-normalized trace-element distribution patterns. Ratios of the source-indicative incompatible elements with the similar distribution coefficients (such as Y-Tb, La-Ta, La-Nb, Dy-Yb, Ba-Nb, Ta-Th, Zr-Hf-Sm, U-Nb-Ta) are practically constant in samples from the Menyailov and Naboko vents. However, some of the fractionation-sensitive element pairs, like Ni-Sc, V-Cr, Zr-Cr, and Ni-Mg, show significant variability: Zr/Cr, V/Cr, Zr/Ti strongly increase in the Menyailov vent lavas, while Ni/Mg, Ni/Sc decrease. Rb/Sr and Ba/Sr remain almost constant independently of the silica content, but are much higher than in the 1975-76 Southern Breakthrough lavas.

Thermodynamic characterization using MELTS (Ghiorso and Sack, 1995; Gualda et al., 2012) of the most primitive bulk rock samples from the Menyailov and Naboko vents shows that predicted liquidus eruption temperatures vary only slightly between the two (T_{liq} ~1148 ºC for Menyailov and 1145 ºC for Naboko; fO_2 fixed at QFM) and are somewhat higher than lava temperatures measured by thermal probes in the field (1080 ºC; Edwards et al., 2014). The predicted liquidus phase for both vents is Pl with liquidus compositions of An59-62 for Menyailov and An62-65 for Naboko samples, followed sequentially by crystallization of Ol, Mt, and Cpx. Non-vesiculated densities for liquidus melt compositions show that the Menyailov lavas are slightly less dense (2580 kg/m^3) than those for the Naboko lavas (2630 kg/m^3).

The 2012-2013 FTE lavas have lower Mg#, higher FeO, TiO_2 and alkali concentrations and higher K_2O/MgO ratios than lavas produced by all of the large stratovolcanoes located in the Central Kamchatka Depression (Klyuchevskoy, Bezymianny, Kamen, Shiveluch: Churikova et al., 2013; Churikova et al., 2001; Ermakov, Vazheevskaya, 1973; Fedotov et al., 1984; Portnyagin et al., 2007; Volynets et al., 1978; Fig. 8). Similar evolution trends are observed in the Ploskye Sopki volcanic massif (Churikova, Sokolov, 1993; Churikova, 1993), although the 2012-2013 FTE products still have higher alkali and Ti concentrations for the same silica contents; several samples of basaltic trachyandesites and trachyandesites from this massif have trace element distribution patterns equal to the newly erupted Tolbachik rocks, but are higher in silica (54.8-57.8 weight percent; Fig. 7A). New data on the major and trace element compositions of rocks produced by Plosky and Ostry Tolbachik stratovolcanoes (Churikova et

al., this issue; Churikova et al., 2014) demonstrate the similarity in composition of the Naboko group rocks to the lavas of the late stage of stratovolcano activity (Churikova et al., 2014; samples from >2100 m a.s.l. on the stratocone's flank), and most of the cinder cones of the monogenetic zone, including the Southern Breakthrough of the GFTE. However, rock compositions of the 2012-13 eruption are more evolved then those of rocks from the 1975-76 Tolbachik fissure eruption and they have systematically lower Mg# then Southern Breakthrough lava at similar Ca/Al ratios (Fig. 8). Trace element distribution patterns in the 2012-2013 Tolbachik fissure eruption rocks are sub-parallel to patterns for the Southern Breakthrough samples (Fig. 7A) and enriched in all incompatible elements, except Sr (Fig. 7B). Therefore, they could be produced by fractionation of Pl from the same parent magma.

4. Discussion

The petrological and geochemical diversity recorded by the 2012-13 Tolbachik eruptive products is subtle after the first three days of the eruption. However, data sets that document the compositional homogeneity throughout 9 months of eruptive activity are important for constraining the range of feasible processes occurring over the timescale of the eruption, the magmatic processes that formed the TD and other monogenetic volcanic fields over time-scales of k.y., and for investigating possible genetic relationships between the Holocene fissure activity of Tolbachinsky Dol and the Plosky Tolbachik stratovolcano. The two principal geochemical questions that have been raised by the 2012-2013 eruption, are: 1) what is the nature of connection between Menyailov and Naboko vent rocks; and 2) what is the nature of the connection (if any) between newly erupted rocks and 1975-76 magmas (high-Mg of the Northern Breakthrough and high-Al of the Southern Breakthrough)? Using major and trace element data together with petrographical and mineralogical observations and thermodynamic modeling, we address these questions below.

4.1. Origins of syn-eruption petrological diversity

Petrographic and geochemical evidence shows that over the course of the eruption a relatively homogeneous batch of magma was erupted. The short-duration chemical diversity at the onset of the eruption could reflect eruption of magma from the boundary zones of the magma storage area, where slight contamination and/or fractionation due to wall rock heat loss is most likely to occur. Liquidus temperatures predicted from bulk rock compositions increase slightly over the duration of the eruption from 1142 ºC to 1151 ºC, which is consistent with progress tapping of more thermally insulated magma over time. The observed Pl compositions range to much higher An-contents (An80) than those predicted for liquidus conditions (An65), while the

groundmass Pl falls within the predicted range (An41-65). This is consistent with the low volume Pl megacrysts having been inherited from a less fractionated magma like that erupted from the Southern Breakthrough in 1975-76 (Volynets et al., 1978; Churikova et al., 2001). Shapes and textures of the microphenocrysts, however, are consistent with equilibrium crystallization from the host magma. Their compositions (e.g. high An content, Fe-Mg zoning), though, might be influenced by the temperature variations caused by self-mixing processes in the magma chamber (Volynets et al., 2015).

The differences in groundmass textures may record changes in the magmatic fO_2, with the fine-grained groundmass having formed when the melt had lower fO_2. If the fO_2 increased just prior to eruption, possibly in the feeder dyke, it could have led to the observed increase in Mt crystallization and larger Mt grains. Other mineralogical data, reported by Volynets et al. (2015), includes documentation of Fe-Mg-An zonation in Pl and compositions of Cpx phenocrysts, which also could result from variations in the oxidation state of the erupting magma. Higher oxygen fugacity prior the eruption is consistent with the increase of Fe at constant Mg concentrations at the edges of Pl microphenocrysts and phenocrysts and lower Ti/Al ratios in Cpx from Menyailov vent lavas compared to the Naboko vent. Hammer (2006) and Del Moro et al. (2013) have suggested that a decrease in Ti/Al in Cpx may signal an fO_2 increase. High-Fo olivines, found in the lavas of the initial stage of the eruption by Izbekov et al. (2014), might also be formed as a response to the sharp increase of the oxygen activity from QFM to NNO and even higher during the fissure opening, in manner analogous to that proposed for the origin of lapilli tuff ejecta at Stromboli volcano, reported by Cortes et al. (2006) and Del Moro et al. (2013).

4.2. Relationship between the Menyailov and Naboko vent samples

Taking into account the similarity of the trace element concentrations in the Menyailov and Naboko groups of vents and the constant elemental ratios, we hypothesize that lavas of these two groups of vents are produced from the same parent magma, fractionated to a different extent. Any other process, such as assimilation of the host rock or involvement of a different magma batch, would cause changes in source-sensitive incompatible element ratios, which is not observed. Furthermore, reported data on the isotopic compositions of the 2012-2013 eruption rocks exclude the possibility of crustal assimilation (Portnyagin et al., this issue; Eremina et al., 2014). Therefore, we argue that the lavas from the Menyailov vents resulted from draining of the upper part of the magma storage zone, which was higher in silica and alkalis and slightly lower in density. The Naboko vent lavas and tephra (located downslope from the Menyailov vent)

formed as the less fractionated, inner part of the magma storage area started to erupt. Involvement of the deeper portions of the magma storage area in the eruption of the Naboko vents is also consistent with the geophysical data (Gordeev et al., 2014). However, involvement of different magma batches at the initial stage of eruption cannot be excluded, as this could be consistent with some petrographic observations of mineral disequilibrium (e.g. Pl with sieve textures). If these batches were more or less similar in composition, differing only in temperature and/or oxygen fugacity, it would not change the chemical composition of products, but might remain imprinted in the microstructure of the rocks (Fig.4D). Otherwise the observed differences in the groundmass textures could be generated directly in the crater area of the vents via recycling of the erupted material through many cycles of ejection and fall/drain-back, although it is unlikely that this process would cause massive Mt crystallization. Furthermore, these two types of groundmass are observed mainly in the rocks of the initial stage of the eruption, before the crater lava pond had formed, so extensive recycling would be less likely.

Simple mass-balance calculations (Fig. 9) show that removal of less than 3 weight percent Mt and ~8 weight percent Cpx produces the observed gap in silica content and change in other major element concentrations reported for Menyailov vent lavas. This hypothesis is supported by the trace element ratio plots (Fig. 9, 10): the only element ratios differing between the Menyailov and Naboko vents rocks are those affected by Mt crystallization – Zr/Ti, Zr/Cr, V/Cr. Decreases in Ni/Sc and Ni/Mg ratios could also be produced by Cpx and Ol crystallization, but here it is caused by Ni depletion in Menyailov magma at almost constant Mg and Sc values. Therefore, fractionation of Mt-Cpx from the magma supplied to the Menyailov vents is the simplest explanation for the chemical variability observed during the first three days of the eruption. The subtle chemical variation during the course of the eruption, including the slight overall increase in Mg#, is consistent with a magma storage zone wherein magma is not strongly chemically zoned but also is not being thoroughly chemically homogenized.

4.3. Constraints on the magma storage area

Estimates of liquidus conditions suggest that between the 1975-76 and the 2012-13 eruptions, the temperature of the accessible high Al basaltic magma within the storage area decreased by ~35˚ C. Fedotov et al. (2011) developed a model for the magma storage area underneath Plosky Tolbachik and its dimensions: they estimated that is has a transverse dimension of ~5 km, a depth of ~3 km, and a volume of 40-60 km^3. Assuming a roughly cylindrical shape to the storage zone with a radius of 2.5 km and a depth of 3 km gives a volume of ~60 km^3. Following the methods outlined for solutions to the Stefan Problem by Turcotte and

Schubert (2002), we have estimated the thickness of a boundary layer of magma that experienced 35˚ of cooling based on the following assumptions for the magma: latent heat of crystallization of 160 kJ/kg (~50 percent crystallization), heat capacity of 1.2 kJ/kg K, and a value of thermal diffusivity of 0.7 x 10^{-6}. After 36 years, a layer of magma ~20 m thick would have cooled ~35˚; given the assumed cylindrical geometry of the storage area, that would generate approximately 0.4 km^3 of magma within the temperature range estimated by our calculations, which is close to the 0.55 km^3 volume estimated for the 2012-13 eruption (Belousov et al., 2015). While these approximations are only order of magnitude calculations, they show that our hypothesized relationship of closed system fractionation between residual magma from the 1975-76 eruption and the 2012-13 basaltic trachyandesite is feasible from a physical perspective.

4.4. Petrogenetic processes in monogenetic volcanic fields

Many fields of monogenetic volcanic cones and flows show evidence for polymagmatic origins, including: Tolbachik, Kamchatka (Volynets et al., 1978; Flerov et al., 1984 and others); the Sredinny Range, Kamchatka (Volynets and Churikova, 2004; Volynets et al., 2010); Jeju Isand, Korea (Brenna et al., 2010; Brenna et al., 2012); Auckland volcanic field, New Zealand (McGee et al., 2012; McGee et al., 2013); Lathrop Wells, Nevada (Perry et al., 1998; Valentine et al., 2007). Chemical variability could be caused by the participation of separate magma batches, which in turn experience a diversity of processes within the source and the conduit systems including varying degrees of melting, different compositions of the source(s), and fractionation of parent melts and assimilation of crust. Practically all parental partial melts are able to exist in an unstable state for some time and subsequently lead to the eruption of chemically different material within a small area and a small time span (McGee et al., 2012). Coexistence of two principally different types of magma (high-Mg, low- to medium-K and high-Al sub-alkaline) in time and space, as it is reported for Klyuchevskoy (e.g., Kersting and Arculus, 1994; Ariskin et al., 1995; Ozerov et al., 1996) and Tolbachik volcanoes and surrounding monogenetic zones (Volynets et al., 1978; Flerov et al., 1984; Hochstaedter et al., 1996; Ermakov and Ermakov, 2006), is interpreted either as a result of fractionation of one parent high-Mg melt to produce the high-Al derivate, or as a result of ascent and/or mixing of two distinct parent magma batches: one generated at greater depth (high-Mg) and the other at lower levels (high-Al).

The chemical variations observed between the 1975-76 and 2012-2013 lavas can be at least partly explained by closed system fractionation of a parent melt with a composition similar to that of the high-Mg magma of the 1975-76 eruption (sample Fed 07, which has the highest

Mg# of Northern Breakthrough samples; Fedotov, 1983). Liquid lines of descent (LLD) calculated using rhyolite-MELTS (Ghiorso and Sack, 1995; Gualda et al., 2012) at low pressures (100-300 MPa , corresponding to a shallow magma storage area between ~3 and 10 km), a fixed fO_2 (QFM), and relatively dry conditions (0-1 weight percent H_2O) are able to reproduce most of the chemical variation seen within the 2012-13 data (Fig. 11). Most of the variations within the high-Mg samples cluster around the starting liquid composition Fed-07. The early part of the crystallization sequence is dominated by Cpx, which depletes the liquid in CaO and MgO, but produces increases in Al_2O_3, K_2O, TiO_2, P_2O_5, all of which are characteristic differences between the high-Mg and high-Al samples from the 1975-76 GTFE. With the exception of Al_2O_3 and K_2O, the modeled LLD's also explain reasonably well both the Menyailov and Naboko sample compositions. While these first cut models do not produce exact matches to the entire data set, they are close enough to be consistent with derivation of all samples erupted in the 1975-76 and 2012-13 from a common ancestral parent melt, with little need for complex models involving multiple sources or significant open-system contamination.

Predicted liquidus temperatures for two of the samples with the highest MgO concentrations from the 1975-6 Southern Breakthrough are 20 ºC higher than those predicted for the 2012-13 samples, and have predicted liquidus compositions for Pl of An69-74. This is consistent with the newly erupted material being derived from remnant high-Al magma from the 1975-6 eruption with only slight amounts of cooling (less than 1 ºC per year) during the intervening 36 years. This scenario implies that within a single field of monogenetic cones, eruptions that produce spatially separate vents and flows over the time-scale of at least decades can either sample related magmas from different storage depths (e.g., Northern versus Southern Breakthroughs), or be repeat samples from the same magma storage area (e.g., 1975-6 Southern Breakthrough and 2012-13 lavas).

5. Conclusions

Our data document the 9-month long eruption of a compositionally homogeneous batch of magma, represented by high alumina basaltic trachyandesites with higher alkalis and titanium concentrations than any previously studied volcanic rocks from Tolbachinsky Dol, on the southern flank of Plosky Tolbachik volcano. The only subtle change of geochemical composition occurred during the first week of the eruption, when the center of activity migrated from the northern (Menyailov) to the southern (Naboko) vents. This process was marked by a drop in SiO_2, K_2O, and Na_2O concentrations as well as the K_2O/MgO ratio, and by increases in MgO, FeO and TiO_2 concentrations. The only trace element ratios affected by this compositional

change are those influenced by Mt crystallization (Zr/Ti, Zr/Cr, V/Cr). We provide evidence that this initial change in geochemistry may be explained by tapping of a slightly cooler and fractionated (approximately 3 % Mt and 8 % Cpx) upper part of the magma storage zone before the main storage area began to feed the eruption.

Chemical variations between the 1975-76 and 2012-2013 eruption products and the predicted liquidus compositions and temperatures for the Southern Breakthrough and 2012-13 samples are consistent with the newly erupted material been derived from the remnant high-Al magma from the 1975-76 eruption with only slight amounts of cooling (less than 1 ºC per year) during the intervening 36 years. Estimates from thermal modeling are permissive for the hypothesized relationship of closed system fractionation between residual magma from the 1975-76 eruption and the 2012-13 basaltic trachyandesite from a physical perspective. Thermodynamic modeling shows that overall variations in 1975-76 and 2012-13 compositions are consistent with a high degree of low pressure (100-300 MPa), relatively dry fractionation of a parent melt compositionally similar to the Northern Breakthrough high-Mg basalts.

The preliminary study of the mineral compositions and groundmass textures of the rocks produced over the course of the eruption uncovered a number of processes that might take place in the magma storage zone prior to and during the eruption (fractionation, self-mixing, oxygen fugacity changes). A detailed study of the mineral zoning, including Fe-Mg diffusion profiling, will provide timescales of crystals' capture and residence, and we consider it to be a very promising direction for future research.

Acknowledgements. We especially thank A. Belousov, M. Belousova, Ya. Muraviev, I. Abkadyrov, D. Saveliev, A. Sokorenko, N. Gorbach, N. Malik for help with the field work and for collecting samples for this study. The authors are grateful to A. Babansky for his help with analytical work, V. Rodin for the sample preparation, and to G. Ponomarev for the consultations on petrography. We thank Ilya Bindeman, anonymous reviewer and a guest editor Alexander Belousov for their thorough reviews, which helped us to improve the earlier version of this manuscript. This work is supported by IVS FEB RAS, RFBR grant 13-05-00760-a, FEB RAS grant no. 12-III-A-08-165 (to A.V.), and a National Science Foundation RAPID 1321648 (to B.E.).

References

Ariskin, A. A., Barmina, G. S., Ozerov, A. Yu., Nielsen, R. L., 1995. Genesis of high-alumina basalts from Klyuchevskoi volcano. Petrol. 3(5), 496-521.

Belousov, A., Belousova, M., Edwards, B., Volynets, A., Melnikov, D., 2015. Overview of the precursors and dynamics of the 2012–13 basaltic fissure eruption of Tolbachik Volcano, Kamchatka, Russia. J. Volcanol. Geotherm. Res. 299, 19-34. doi:10.1016/j.jvolgeores.2015.04.009

Brenna, M., Cronin S. J., Smith I. E., Maas R., Sohn Y. K., 2012. How small-volume basaltic magmatic systems develop: a case study from the Jeju Island Volcanic Field, Korea. J. Petrol. 53 (5), 985-1018. doi:10.1093/petrology/egs007.

Brenna, M., Cronin, S. J., Smith, I. E., Sohn, Y. K., Németh, K., 2010. Mechanisms driving polymagmatic activity at a monogenetic volcano, Udo, Jeju Island, South Korea. Contrib. Miner. Petrol. 160(6), 931-950.

Churikova, T.G., 1993. Geochimia i modelirovanie magmaticheskogo processa vulkanov Klyuchevskoy gruppy. Ph.D. Thesis. Lomonosov's Moscow State University, Moscow, Russia (in Russian).

Churikova, T.G., Sokolov, S.Yu., 1993. Magmatic evolution of Ploskye Sopki volcano, Kamchatka (analyses of strontium isotope geochemistry). Geochem. Intern. 10, 1439-1448 (in Russian with English abstract).

Churikova, T.G., Gordeychik, B.N., Edwards, B.R., Ponomareva, V.V., Zelenin, E., 2015. The Tolbachik volcanic complex: a review of the petrology, volcanology and eruption history prior to the 2012–2013 eruption. J. Volcanol. Geotherm. Res. (this issue).

Churikova, T., Gordeichik, B., Iwamori, H., Nakamura, H., Nishizawa, T., Haraguchi, S., Yasukawa, K., Ishizuka, O., 2014. Petrology and geochemistry of the Tolbachik stratovolcano. Proceedings of the 8th Biennial Workshop on Japan-Kamchatka-Alaska Subduction Processes: Finding clues for science and disaster mitigation from International collaboration (JKASP-2014). Hokkaido University, Sapporo, Japan. http://hkdrcep.sci.hokudai.ac.jp/map/jkasp2014/proglist.html.

Churikova, T. G., Gordeychik, B. N., Ivanov, B. V., Wörner, G., 2013. Relationship between Kamen Volcano and the Klyuchevskaya group of volcanoes (Kamchatka). J. Volcanol. Geotherm. Res. 263, 3-21.

Churikova, T., Dorendorf, F., Woerner, G., 2001. Sources and fluids in the mantle wedge below Kamchatka, evidence from across-arc geochemical variation. J. Petrol. 42, 1567-1593. doi:10.1093/petrology/42.8.1567

Cortes, J.A., Wilson, M., Condliffe, E., Francalanci, L., 2006. The occurrence of forsterite and highly oxidizing conditions in basaltic lavas from Stromboli volcano, Italy. J. Petrol. 47 (7), 1345-1373.

Del Moro, S., Renzulli, A., Landi, P., La Felice, S., Rosi, M., 2013. Unusual lapilli tuf ejecta erupted at Stromboli during 15 March 2007 explosion shed light on the nature and thermal state of rocks forming the crater system of the volcano. J. Volcanol. Geotherm. Res. 254, 37-52.

Dvigalo, V. N., Svirid, I. Yu., Shevchenko, A. V., 2014. The first quantitative estimates of parameters for the Tolbachik Fissure Eruption of 2012-2013 from aerophotogrammetric observations. J. Volcanol. Seismol., 8(5), 261-268. doi: 10.1134/S0742046314050029

Edwards, B.R., Belousov, A., Belousova, M., 2014. Propagation style controls lava-snow interactions. Nat. Commun. 5:5666, doi: 10.1038/ncomms6666.

Eremina, T.S., Khubunaya, S.A., Koloskov, A.V., Moskaleva, S.V., 2014. Izvestkovo-shhelochnye i subshhelochnye bazal'ty i andezibazal'ty vulkanov Klyuchevskoy, Harchinskiy i Ploskiy Tolbachik (TTI-50) — vulkanicheskie produkty raznoglubinnoj mantii. Proceedings of the annual conference on Volcanologists day “Volcanism and related processes”. IVS FEB RAS, Petropavlovsk-Kamchatsky, pp. 207-211 (in Russian).
http://www.kscnet.ru/ivs/publication/volc_day/2014/art11.pdf

Ermakov, V.A., Ermakov, A.V., 2006. Geological-petrological models of the 1975-1976 eruption at Tolbachinsky Dol (Klyuchevskoy group of volcanoes). Geophysical Research. 5, 53-115 (in Russian).

Ermakov, V.A., Vazheevskaya, A.A., 1973. Vulkany Ostry and Plosky Tolbachik. Bulletin volcanologicheskih stantsij AN SSSR 49, 36-43 (in Russian).

Hammer, J.E., 2006. Influence of fO_2 and cooling rate on the kinetics and energetic of Fe-rich basalt crystallization. Earth Planet. Sci. Lett. 248, 618-637.

Hochstaedter, A. G., Kepezhinskas, P., Defant, M., Drummond, M., Koloskov, A., 1996. Insights into the volcanic arc mantle wedge from magnesian lavas from the Kamchatka arc. J. Geophys. Res.: Solid Earth (1978–2012), 101(B1), 697-712.

Izbekov, P., Koloskov, A., Maximov, A., Khabunaya, S., 2014. The 2012 Fissure Tolbachik eruption: preliminary results of petrological investigation // Geophys. Res. Abstr. Vol.

16, 2014 EGU General Assembly, Vienna, http://meetingorganizer.copernicus.org/EGU2014/EGU2014-11710.pdf.

Fedotov, S.A. (Ed.), 1983. The Great Tolbachik Fissure Eruption; geological and geophysical data 1975-1976. Cambridge Univ. Press, Cambridge, United Kingdom. 353 p.

Fedotov, S.A., Utkin, I.S., Utkina, L.I., 2011. The peripheral magma chamber of Ploskii Tolbachik, a Kamchatka basaltic volcano: activity, location and depth, dimensions, and their changes based on magma discharge observations. J. Volcanol. .Seismol. 5, 369-385. doi: 10.1134/S0742046311060042

Fedotov, S.A., Balesta, S.T., Dvigalo, V.N., Razina, A.A., Flerov, G.B., Chirkov, A.M., 1991. New Tolbachik volcanoes. In: Fedotov S.A., Balesta S.T., Masurenkov Yu.P. (Eds.), Active volcanoes of Kamchatka. Nauka, Moscow. Vol.1, pp. 214-279 (in Russian with English abstract).

Fedotov, S.A., Flerov, G.B., Chirkov, A.M. (eds.), 1984. The 1975-1976 Large Tolbachik Fissure Eruption in Kamchatka. Nauka, Moscow (in Russian with English abstract).

Flerov, G. B., Andreev, V. N., Budnikov, V. A., Tsyurupa, A. I., 1984. Petrology of the eruption products. In: Fedotov S.A., Flerov G.B., Chirkov A.M. (eds.), 1984. The 1975-1976 Large Tolbachik Fissure Eruption in Kamchatka. Nauka, Moscow (in Russian with English abstract). P. 223-276.

Gordeev, E. I., Droznin, V. A., Dubrovskaya, I. K., Dvigalo, V. N., Maguskin, M. A., Muravyev, Ya. D., Titkov, N. V., Volynets, A. O., 2014. Fissure eruption on Tolbachik Dol (FTE-50, Kamchatka, 2012-2013). Proceedings of the 8th Biennial Workshop on Japan-Kamchatka-Alaska Subduction Processes: Finding clues for science and disaster mitigation from International collaboration (JKASP-2014). Hokkaido University, Sapporo, Japan. http://hkdrcep.sci.hokudai.ac.jp/map/jkasp2014/proglist.html.

Ghiorso, M.S., Sack, R.O., 1995. Chemical mass transfer in magmatic processes. IV. A revised and internally consistent thermodynamic model for the interpolation and extrapolation of liquid-solid equilibria in magmatic systems at elevated temperatures and pressures. Contrib. Mineral. Petrol. 119, 197-212.

Gualda, G. A. R., Ghiorso, M. S., Lemons, R. V., Carley, T. L., 2012. Rhyolite-MELTS: A modified calibration of MELTS optimized for silica-rich, fluid-bearing magmatic systems. J. Petrol. 53, 875-890.

Karandashev, V. K., Turanov, A. N., Orlova, T. A., Lezhnev, A. E., Nosenko, S. V., Zolotareva, N. I., Moskvitina, I. R., 2008. Use of the inductively coupled plasma mass spectrometry for element analysis of environmental objects. Inorg. Mater. 44, 1491-1500.

Kersting, A. B., Arculus, R. J., 1994. Klyuchevskoy volcano, Kamchatka, Russia: the role of high-flux recharged, tapped, and fractionated magma chamber (s) in the genesis of high-Al_2O_3 from high-MgO basalt. J. Petrol. 35(1), 1-41.

Kugaenko, Yu., Titkov, N. Saltykov, V., 2015. Constraints on unrest in the Tolbachik volcanic zone in Kamchatka prior the 2012-13 flank fissure eruption of Plosky Tolbachik volcano from local seismicity and GPS data. J. Volcanol. Geotherm. Res. (this issue).

Le Maitre, R.W. (Ed.), 1989. A classification of the igneous rocks and glossary of terms. Recommendations of the International Union of Geological Sciences on the systematics of igneous rocks. Oxford: Blackwell Scientific Publications.

McGee, L. E., Smith, I. E., Millet, M. A., Handley, H. K., Lindsay, J. M., 2013. Asthenospheric control of melting processes in a monogenetic basaltic system: A case study of the Auckland Volcanic Field, New Zealand. J. Petrol. 54 (10), 2125-2153. doi: 10.1093/petrology/egt043.

McGee, L. E., Millet, M. A., Smith, I. E., Németh, K., Lindsay, J. M., 2012. The inception and progression of melting in a monogenetic eruption: Motukorea Volcano, the Auckland Volcanic Field, New Zealand. Lithos 155, 360-374. doi: 10.1016/j.lithos.2012.09.012

Melnikov, D., Volynets, A., (in review). Remote sensing and petrological observations on the 2012-2013 fissure eruption at Tolbachik volcano, Kamchatka: implications to the reconstruction of the eruption chronology. J. Volcanol. Geotherm. Res. (this issue).

Ozerov, A. Y., Ariskin, A. A., Barmina, G. S., 1996. The Problem of Genetic Relations between High-Aluminous and High-Magnesian Basalts of the Klyuchevskoi Volcano, Kamchatka. Transactions of the Russian Academy of Sciences-Earth Science Sections, 350(7), 1127-1130.

Perry, F. V., Crowe, B. M., Valentine, G. A., Bowker, L. M. (Eds.), 1998. Volcanism studies: final report for the Yucca Mountain project. Los Alamos National Laboratory Report LA-13478-MS. 554 pp.

Portnyagin, M., Duggen, S., Hauff, F., Mironov, N., Bindeman, I., Thirlwall, M., Hoernle, K., 2015. Geochemistry of the Late Holocene rocks from the Tolbachik volcanic field, Kamchatka: towards quantitative modeling of subduction-related open magmatic systems. J. Volcanol. Geotherm. Res. (this issue).

Portnyagin, M., Bindeman, I., Hoernle, K., Hauff, F., 2007. Geochemistry of primitive lavas of the Central Kamchatka Depression: Magma generation at the edge of the Pacific Plate. In: Eichelberger J., Gordeev E., Izbekov P., Kasahara M., Lees J. (Eds.) Volcanism and Subduction: The Kamchatka Region. Washington D.C.: AGU, 2007. V. 172, pp. 203-244. doi: 10.1029/172GM16

Russell, J. K., Hauksdottir, S., 2000. Estimates of crustal assimilation in Quaternary lavas from the northern Cordillera, British Columbia. Canad. Mineral. 39, 275-297.

Senyukov, S.L., Nuzdina, I.N., Droznina, S.Ya, Garbuzova, V.T., Kozhevnikova, T.Yu, Sobolevskaya, O.V., Nazarova, Z.A., Bliznetsov, V.E., 2015. Seismic monitoring of the Plosky Tolbachik eruption in 2012–13 (Kamchatka Peninsula, Russia). J. Volcanol. Geotherm. Res. (this issue).

Sun, S.S., McDonough, W.F., 1989. Chemical and isotopic systematic of oceanic basalts; implications for mantle composition and processes. Geol. Soc. Lond. Spec. Publ. 42, 313-345.

Tatsumi, Y., Kogiso, T., Nohda, S., 1995. Formation of a third volcanic chain in Kamchatka: generation of unusual subduction-related magmas. Contrib. Mineral. Petrol., vol. 120, 117-128.

Turcotte, D. L., Schubert, G., 2002. Geodynamics. Cambridge University Press, Cambridge, 456 p.

Valentine, G. A., Krier, D. J., Perry, F. V., Heiken, G., 2007. Eruptive and geomorphic processes at the Lathrop Wells scoria cone volcano. J. Volcanol. Geotherm. Res. 161(1–2), 57–80

Volynets, A., Griboedova, I., 2015. Zonal'nost' v plagioklazah Treshhinnogo Tolbachinskogo izverzhenija 2012-2013. v svyazi s processami v magmaticheskoy kamere. Proceedings of the annual conference on Volcanologists day “Volcanism and related processes”. IVS FEB RAS, Petropavlovsk-Kamchatsky (In Russian). http://www.kscnet.ru/ivs/conferences/documents/tezis_2015.pdf

Volynets, A., Melnikov, D., 2013. Rekonstrukcija perioda nachala Treshhinnogo Tolbachinskogo izverzhenija imeni 50-letija IViS DVO RAN po petrologicheskim i sputnikovym dannym. Proceedings of the annual conference on Volcanologists day "Volcanism and related processes". IVS FEB RAS, Petropavlovsk-Kamchatsky, pp.14-15 (in Russian)

Volynets A.O., Churikova T.G., 2004. Heterogeneity of mantle source of Later Pleistocene-Holocene monogenetic volcanism in Sredinny Ridge of Kamchatka. // Linkages between tectonic, seismicity, magma generation and volcanoes eruption in volcanic arcs: Abstracts of the IV Biennial Workshop on Subduction Processes emphasizing the Japan-Kurile-Kamchatka-Aleutian Arcs. Petropavlovsk-Kamchatsky, p.125-127. http://kiska.giseis.alaska.edu/kasp/kasp04/abstracts/volynets.pdf

Volynets, A., Melnikov, D., Griboedova, I., 2014a. Plagioclase lapilli and phenocrysts in the lavas of the 2012-2013 Tolbachik Fissure eruption. Proceedings of the 8th Biennial Workshop on Japan-Kamchatka-Alaska Subduction Processes (JKASP-2014): Finding clues for science and disaster mitigation from International collaboration. Hokkaido University, Sapporo, Japan. http://hkdrcep.sci.hokudai.ac.jp/map/jkasp2014/proglist.html.

Volynets, A. O., Melnikov, D. V., Yakushev, A. I., Griboedova, I. G., 2014b. Treschinnoe Tolbachinskoe izverzhenie 2012-2013: pervie dannie o variacijah sostava porod, vkraplennikov i kristallolapillej plagioclaza. Proceedings of the annual conference on Volcanologists day "Volcanism and related processes". IVS FEB RAS, Petropavlovsk-Kamchatsky, pp. 32-37 (in Russian). http://www.kscnet.ru/ivs/publication/volc_day/2014/art5.pdf

Volynets, A. O., Melnikov, D. V., Yakushev, A. I., 2013. First data on composition of the volcanic rocks of the IVS 50th anniversary Fissure Tolbachik eruption (Kamchatka). Dokl. Earth Sci. 452(1), 953-957. doi: 10.1134/S1028334X13090201

Volynets, A., Churikova, T., Wörner, G., Gordeychik, B., Layer, P., 2010. Mafic Late Miocene - Quaternary volcanic rocks in the Kamchatka back arc region: implications for subduction geometry and slab history at the Pacific-Aleutian junction. Contrib. Miner. Petrol. 159, 659–687. doi: 10.1007/s00410-009-0447-9.

Volynets, O. N., Babanskii, A. D., Gol'tsman, Y. V., 2000. Variations in isotopic and trace-element composition of lavas from volcanoes of the Northern group, Kamchatka, in relation to specific features of subduction. Geochem. Int. 38 (10), 974-989.

Volynets, O. N., Flerov, G. B., Andreev, V. N., Popolitov, E. I., Abramov, V. A., Petrov, L. P., Scheka, S. A., 1978. Petrochimia, geochimia and voprosi genesisa porod Bolshogo Treschinnogo Tolbachinskogo izverzhenia 1975-76 gg. Dokl. Akad. Nauk SSSR 238 (4), 940-943 (in Russian).

FIGURE and TABLE CAPTIONS

Table 1. Major and trace element concentrations in samples from the 2012-2013 Tolbachik fissure eruption (results of XRF analyses). Concentrations of major oxides in weight percent and of minor and trace elements in ppm. L – lava, B – bomb, S – scoria. Samples from the Menyailov vents are marked by italics in the "Sample No" column.

Table 2. Concentrations of trace elements in the rocks of the 2012-2013 Tolbachik fissure eruption (in ppm). Samples analyzed in GZG, Georg-August Universität Göttingen, are marked by bold type in the "Sample No" column; Menyailov vent lava samples are marked by italics. L – lava, B – bomb, S –scoria.

Fig. 1. Schematic map showing the distribution of the 2012-2013 Tolbachik eruption lava flows and location of the adjacent volcanoes. Legend: 1 – Menyailov vents and lava flows; 2 – Naboko vents and lava flows; 3 – Menyailov lava flows that were later mostly buried by the Naboko lavas; 4 – sampling sites; 5 – location of centers of activity. This map is derived from TERRA, ASTER (NASA, JPL), and EO-1 ALI (NASA) satellite image interpretations and field observations. The topographic base is a DEM-derived from SRTM X-band (DLR). Details of sampling with coordinates in WGS84 geographic projection can be found in the supplementary material. *Full page width.*

Fig. 2. Photographs of typical hand samples from the 2012-2013 Tolbachik eruption. Sample Tolb1201 is from a lava flow erupted from the Menyailov vents on November 27th, 2012; sample Tolb1315 was erupted on April 26th 2013, and was collected from the inner part of a lava flow from the Naboko vents. *Full page width.*

Fig. 3. Backscatter secondary electron (BSE) images of phenocryst phases in samples from the Naboko vents: A) Pl megacryst fragment; B) microphenocrysts of Pl; C) and D) microphenocrysts of Ol. Images are from samples To-17 (A, B) and To-19 (D), which were collected on February 9th , and Tolb-1317/2 (C), which was collected on August 16th, 2013. *Full page width.*

Fig. 4. BSE images of the groundmass in samples from the Naboko vent lavas: A) Intersertal texture in sample TOLB-1315 collected on 26th April, 2013 from the massive internal part of the lava flow; B) and C) hyaline and hyalopilitic textures in sample To-17 collected on February 9th, 2013 from outer part of the lava flow, sampled from a flowing lava channel; D) sharp contact between groundmass with two textures in sample Tm5 collected on December 2nd, 2012, from the front of a distal lava flow from the source main vent. *One and a half column width.*

Fig. 5. Harker diagrams showing the compositional variation in samples from the 2012-2013 and 1975-76 Tolbachik fissure eruption rocks. Legend: 1-2 - 2012-2013 Tolbachik fissure eruption rocks: 1 – samples from Menyailov vents, 2 – samples from Naboko vents; 3-4 – samples from 1975-76 Tolbachik fissure eruption: 3 – Southern Breakthrough, 4 – Northern Breakthrough. Compositions of 1975-76 volcanic rocks are from Churikova et al. (2001), Fedotov (1983), Fedotov et al. (1984), Portnyagin et al. (2007), Volynets et al. (1978), Volynets et al. (2000), and Tatsumi et al. (1995). Discrimination lines on the K_2O - SiO_2 and $K_2O + Na_2O$ - SiO_2 diagrams are from Le Maitre (1989). *One and a half column width.*

Fig. 6. Temporal variations in sample compositions over the course of the eruption. The horizontal axis represents time. Black symbols are samples from the Menyailov vents, white symbols are samples from the Naboko vent. *Full page width.*

Fig. 7. Variations in normalized trace element concentrations. A) Trace element concentrations for the volcanic rocks of the 2012-2013 Tolbachik fissure eruption, 1975-76 Tolbachik fissure eruption and high-K andesites of Ploskye Sopki volcanic massif, normalized to primitive mantle (normalization values from Sun and McDonough, 1989); 1-2 - 2012-2013 Tolbachik fissure eruption: 1 – samples from Menyailov vents, 2 – samples from Naboko vents; 3-4 - 1975-76 Tolbachik fissure eruption rocks: 3 – Southern Breakthrough, 4 – Northern Breakthrough; 5 – high-K andesites of Ploskye Sopki volcanic massif. B) Trace element concentrations in the volcanic rocks of the 2012-2013 Tolbachik fissure eruption, normalized to a Southern Breakthrough basalt (sample 22-8, Mg#=45.62; concentrations of trace elements reported in Churikova et al., 2001); 1 – samples from Menyailov vents, 2 – most silica-rich sample Tm-8 (SiO_2 = 55.35 wt. %); 3 – samples from Naboko vents. *Single column width.*

Fig. 8. K_2O vs. SiO_2, molar Ca/Al vs. Mg#, and K_2O/MgO vs. TiO_2 diagrams for the 2012-2013 Tolbachik fissure eruption rocks compared to the rocks from the Klyuchevskoy volcano group and Ploskye Sopki massif. Legend: 1-2 - 2012-2013 Tolbachik fissure eruption rocks: 1 – samples from Menyailov vents, 2 – samples from Naboko vents; 3 – 6 – samples from CKD volcanoes: 3 – samples from Shiveluch, 4 – samples from Klyuchevskoy, 5 - samples from Kamen, 6 – samples from Bezymianny; fields: 7 - Mg basalts of Tolbachinsky Dol, including 1975-76 fissure eruption; 8 - Al-basalts and basaltic andesites of Tolbachinsky Dol, including 1975-76 fissure eruption; 9 - Plosky and Ostry Tolbachik stratovolcanoes; 10 - Ploskye Sopki volcanic massif. Compositions of TD volcanic rocks from Churikova et al. (2001), Fedotov, (1983), Fedotov et al. (1984), Portnyagin et al. (2007), Volynets et al. (2000), Volynets et al. (1978); Plosky and Ostry Tolbachik from Portnyagin et al. (2007), Ermakov, Vazheevskaya, (1973), Ploskye Sopki from Churikova (1993), Churikova, Sokolov (1993); Klyuchevskoy, Kamen, Bezymianny, Shiveluch from Churikova et al. (2013); Churikova et al. (2001), Portnyagin et al. (2007). Discrimination lines on K_2O - SiO_2 diagram from Le Maitre (1989). *Single column width.*

Fig. 9. Petrogenetic relationships between Menyailov and Naboko vent samples. Variations in Sr/Ni for samples from the Menyailov and Naboko vents compared to a simple fractionation model line (F - fractionation degree). Symbols as in Fig. 5. A ratio of Cpx:Mt of 3:1 was used for the fractionation model based on mass ratios of these two phases predicted to crystallize from rhyolite-MELTS over the temperature range encompassed by Menyailov and Naboko samples, and which is approximately the proportions for best fit mass balance models for major elements

(inset; based on mass balance model from Russell and Hauksdottir, 2000). Ellipses represent 1, 2 and 3 sigma errors (inner, intermediate and outer ellipses respectively) for the calculations based on the indicated samples: Tolb1201 and TM08 are lava samples from the Menyailov group of vents, TM05 is a lava sample from the Naboko groups of vents, erupted at the first week of December, D1307 is a representative sample of the Naboko group of vents, Naboko average is an averaged composition from 64 samples of lava, erupted from the middle December until the end of the event. *One and a half column width.*

Fig. 10. Trace element ratios in samples from the 2012-2013 and 1975-76 Tolbachik fissure eruptions rocks. Note that for the Zr/Cr and V/Cr vs. SiO_2 plots a logarithmic scale for the ordinate axis is used for better presentation of the data. Symbols as in Figure 5. *One and a half column width.*

Fig. 11. Harker diagrams for the samples from the 2012-2013 and the 1975-76 Tolbachik fissure eruptions, comparing model LLDs from rhyolite-MELTS with the observed compositions; all LLDs were calculated at a pressure of 100 MPa. Legend: 1 – fractional crystallization (1 % H_2O); 2 – fractional crystallization (anhydrous); 3 – equilibrium crystallization (1 % H_2O). Other symbols as in Figure 5. See text for discussion. *One and a half column width.*

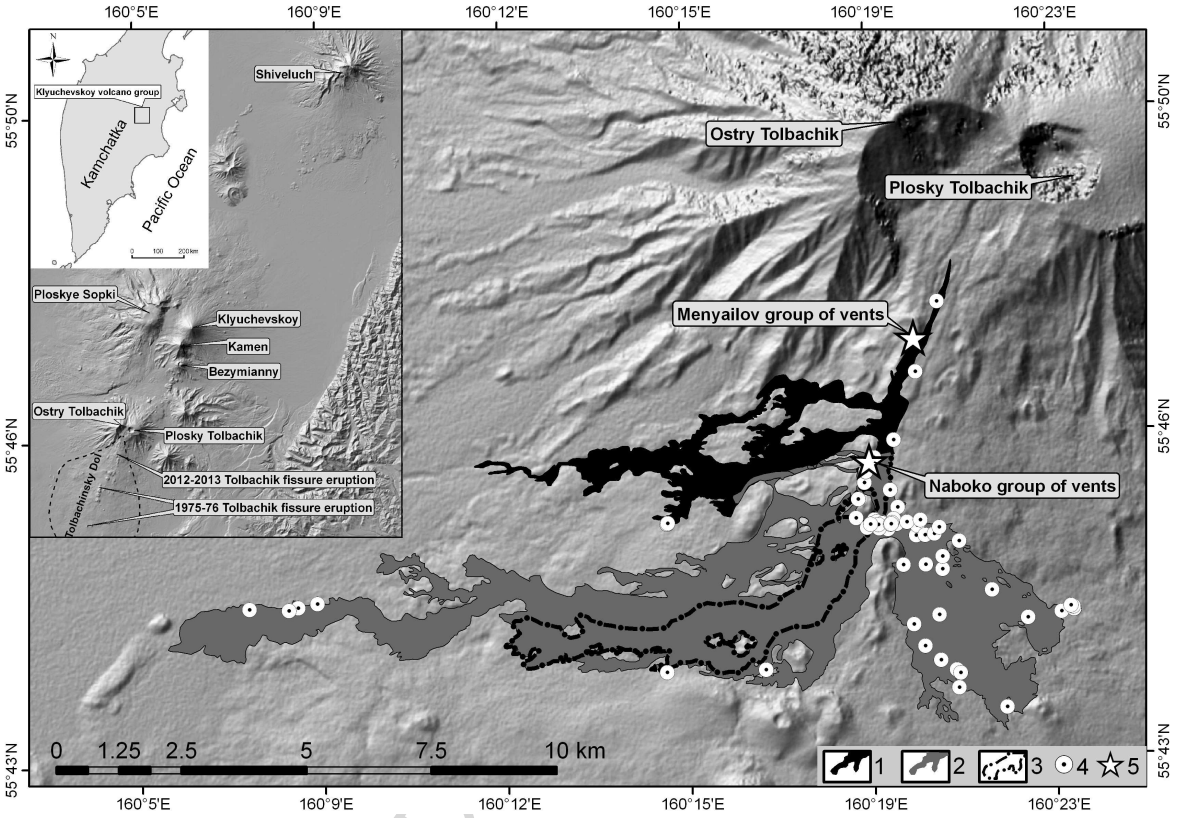

Figure 1

Figure 2

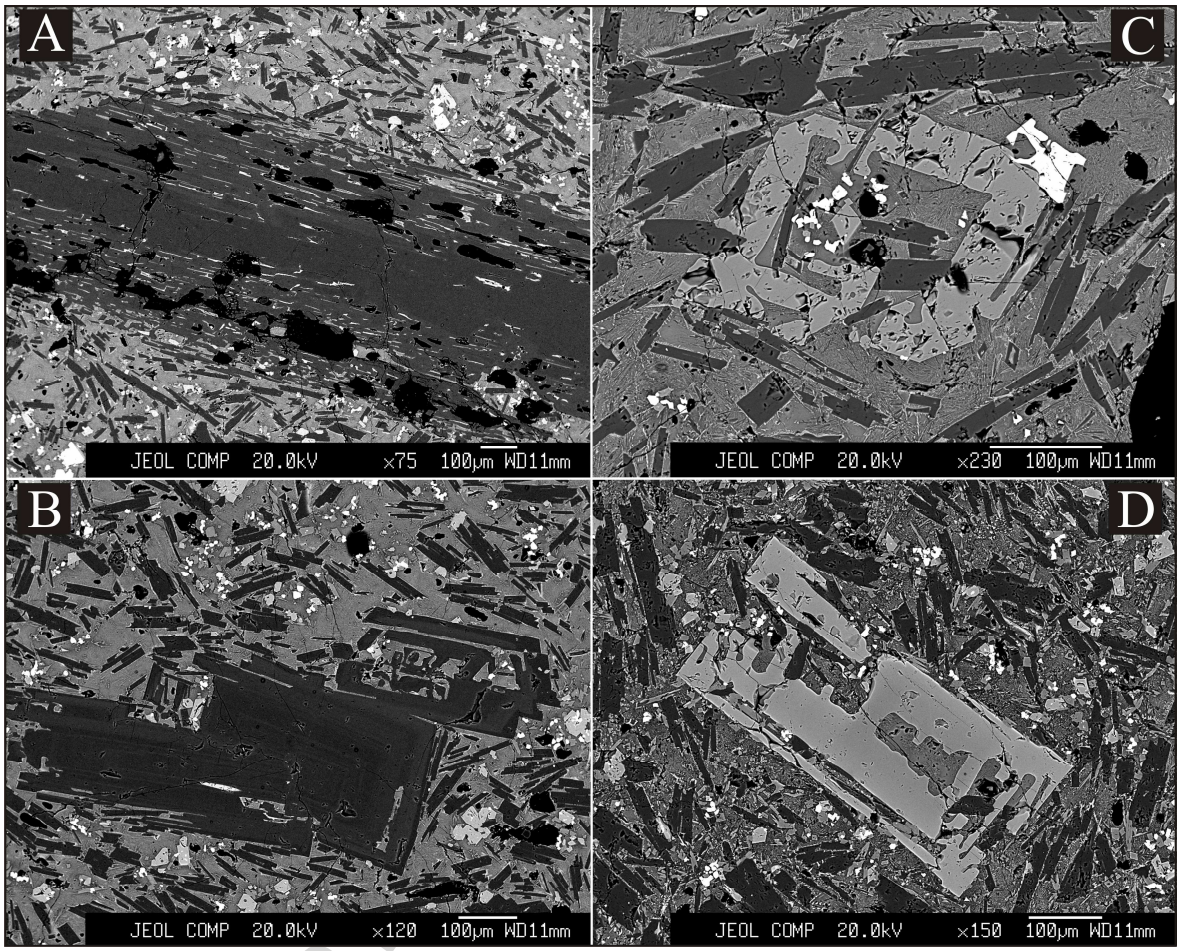

Figure 3

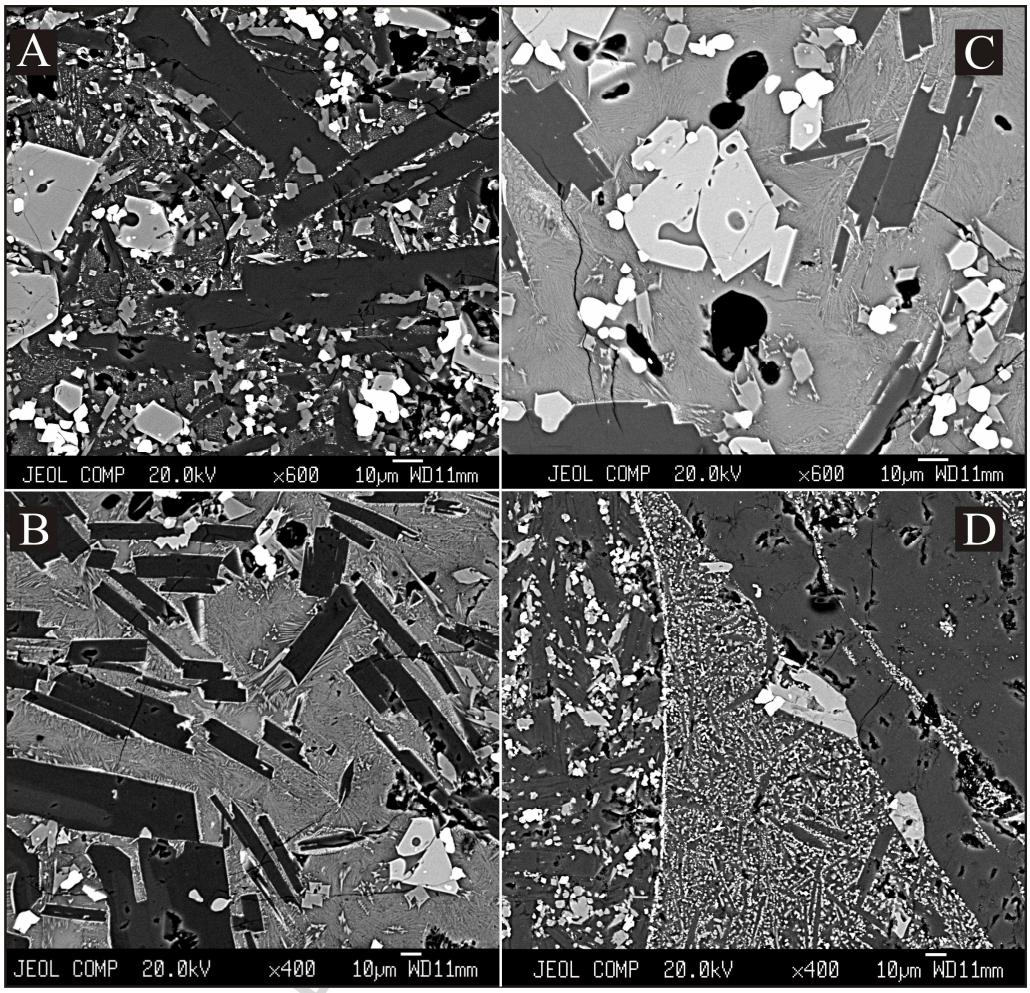

Figure 4

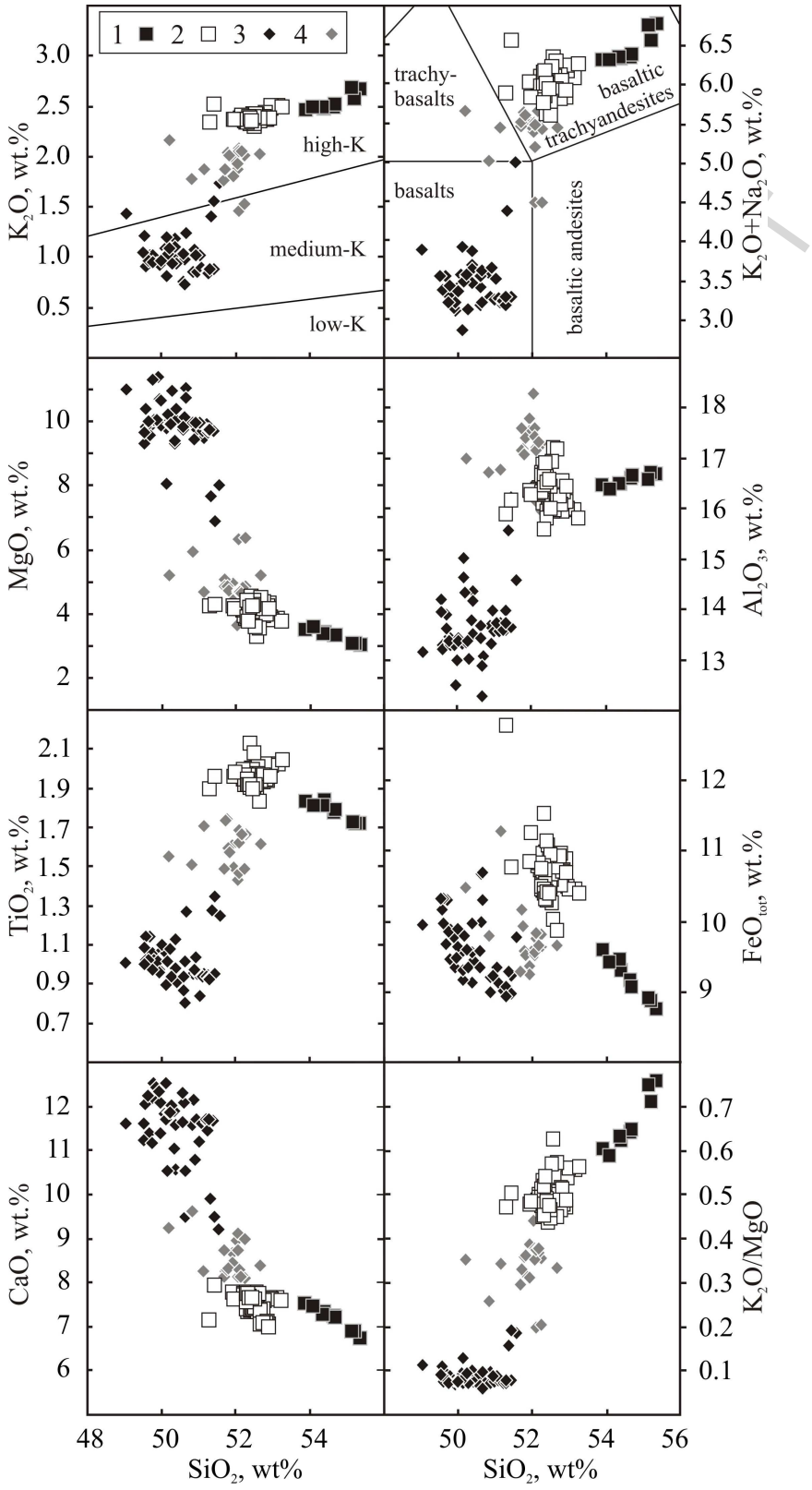

Figure 5

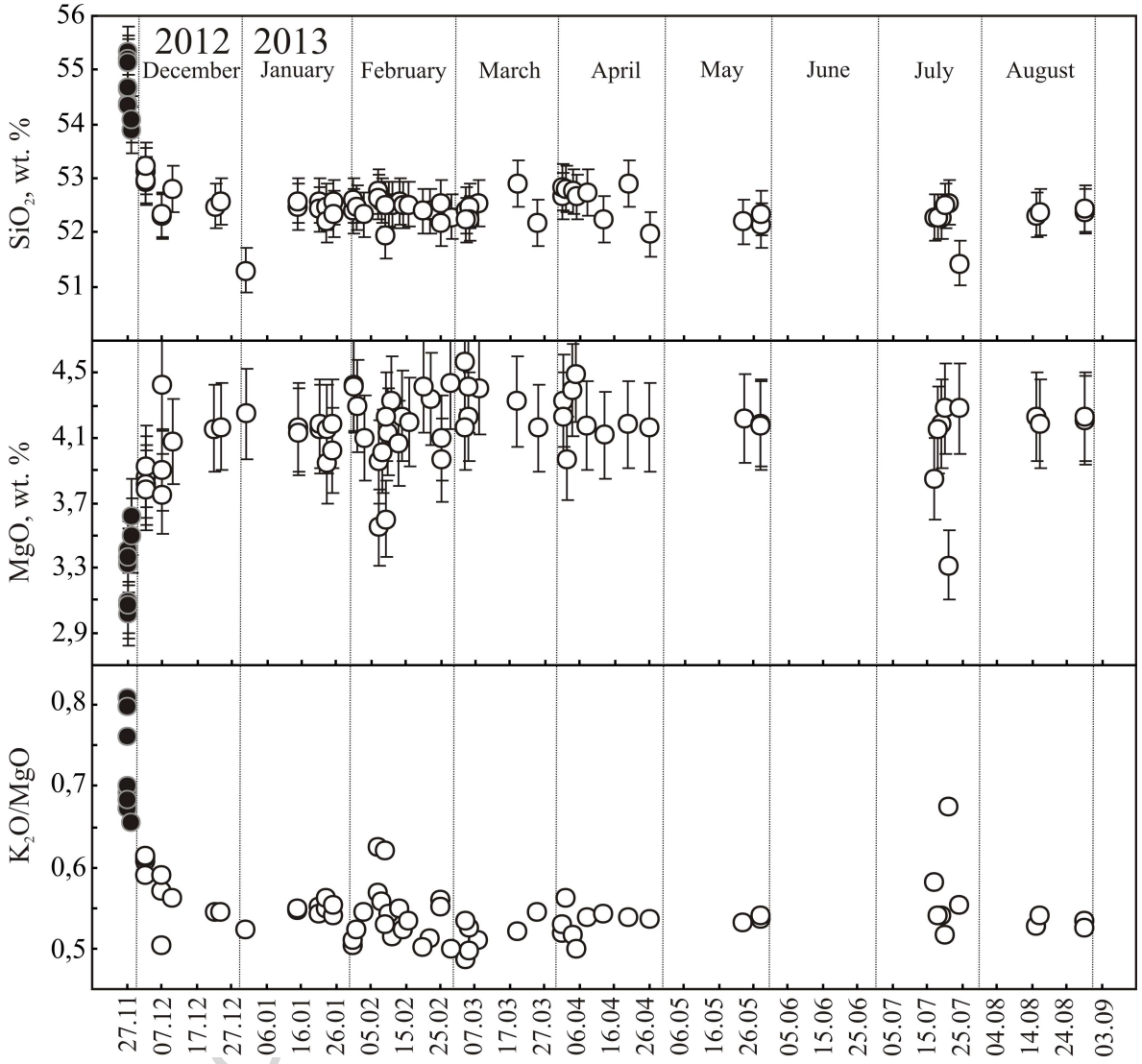

Figure 6

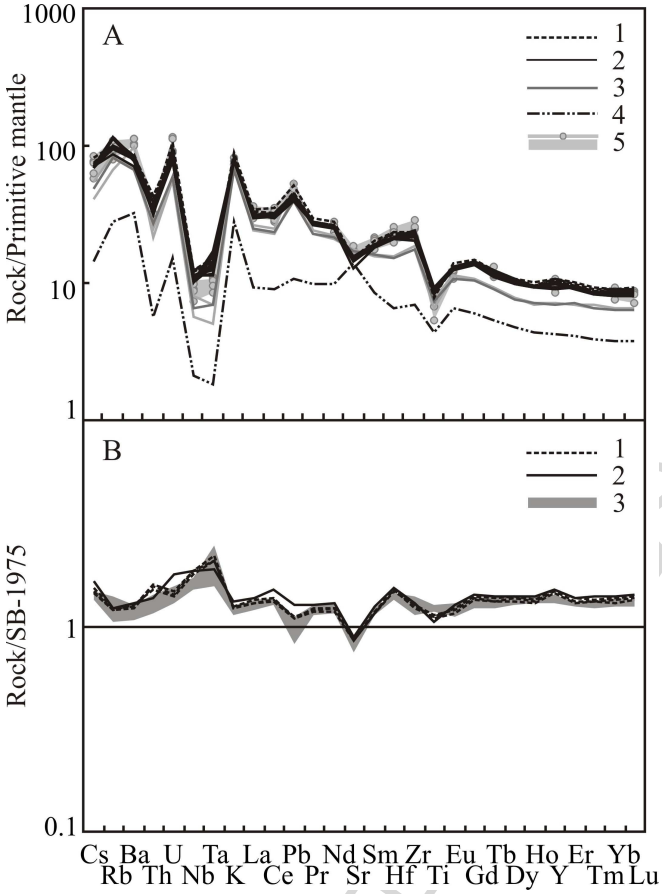

Figure 7

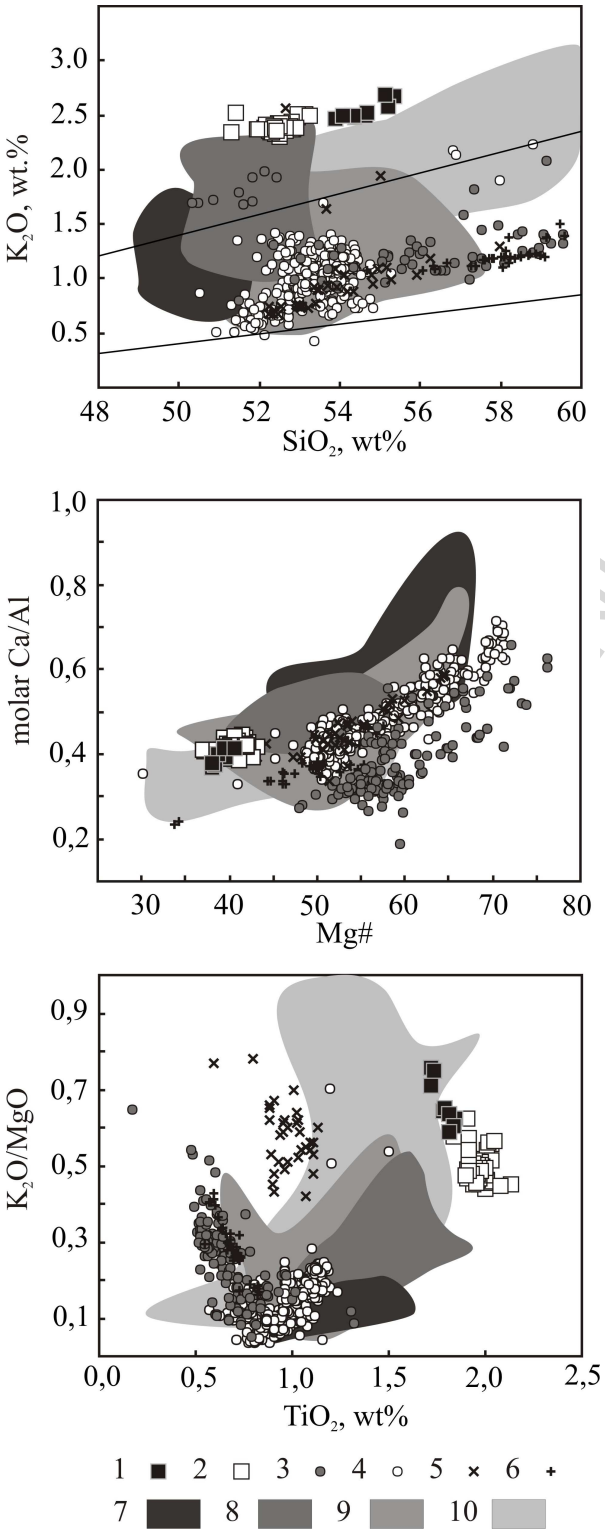

Figure 8

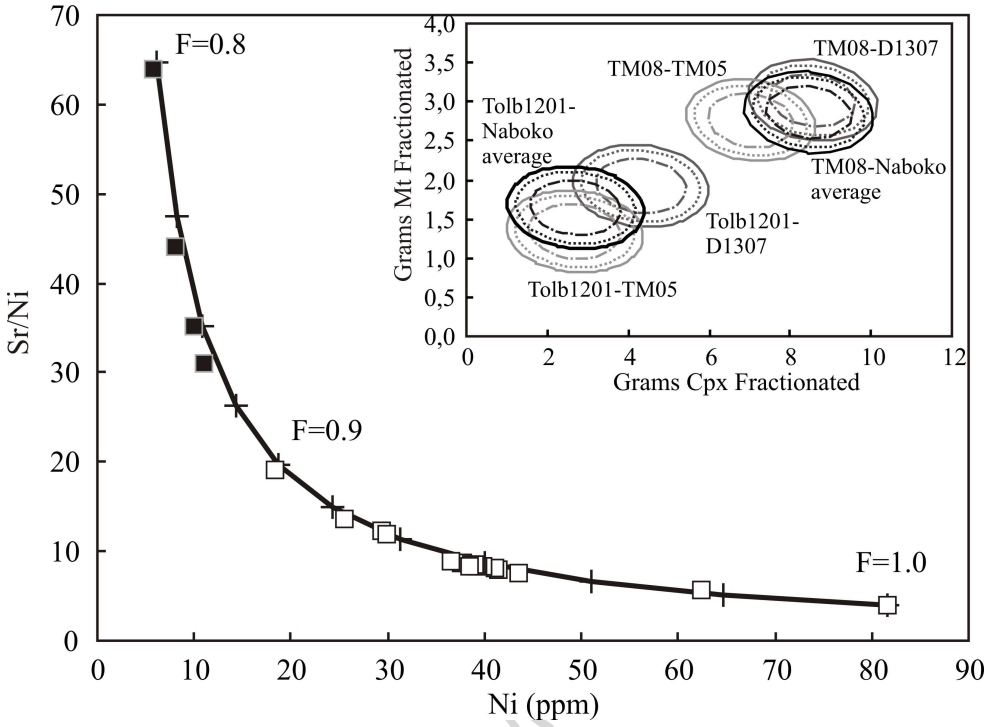

Figure 9

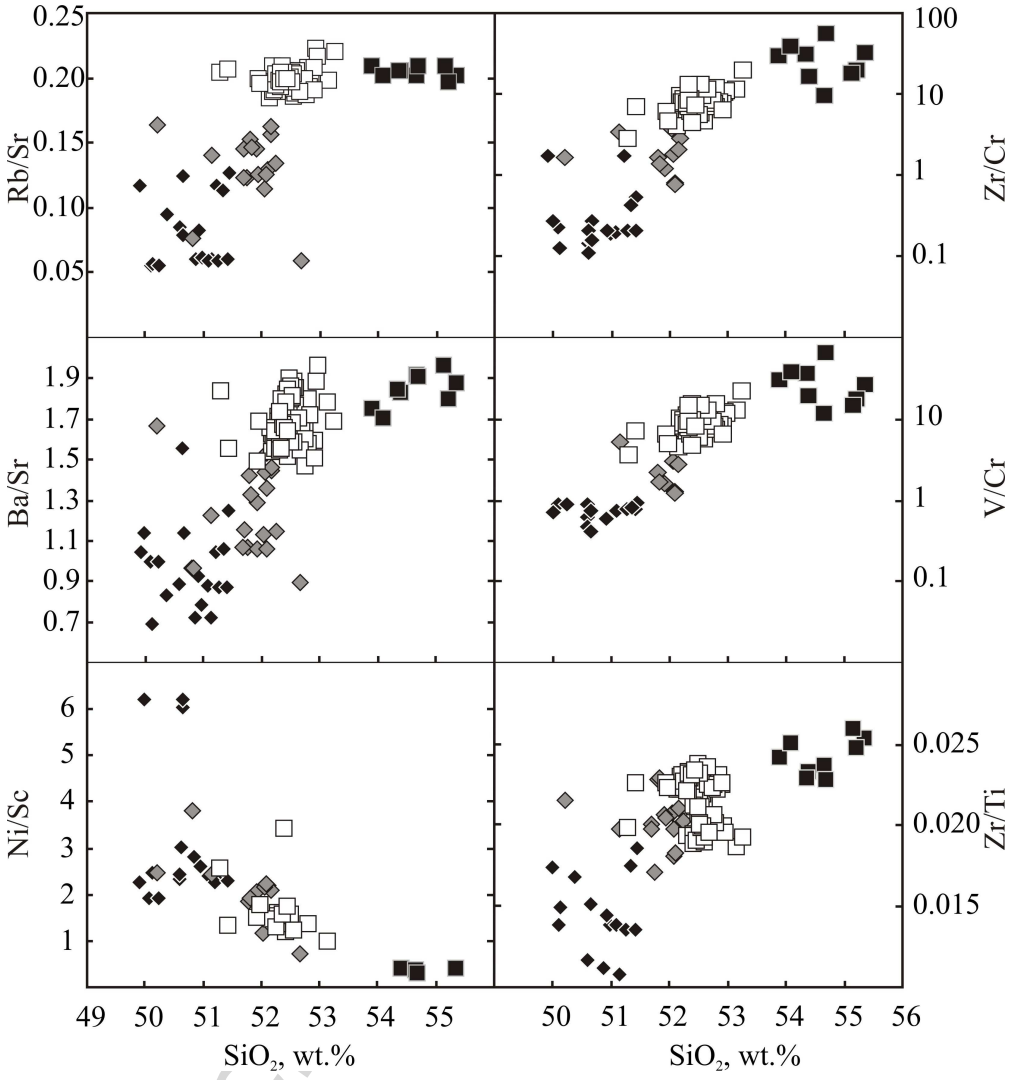

Figure 10

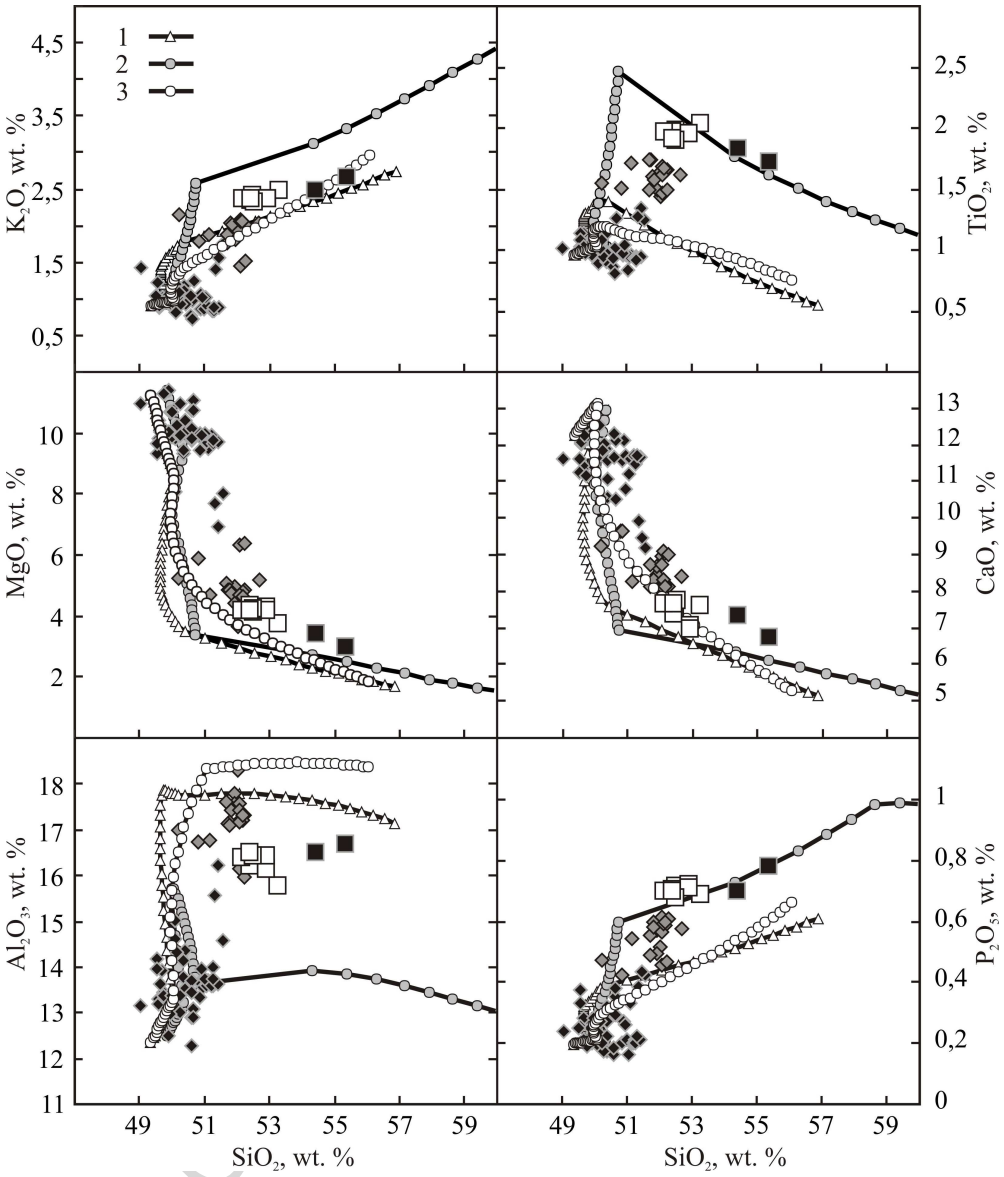

Figure 11

Table 1. Major and trace element concentrations in the FTE volcanic rocks (results of XRF analyses). Concentrations of major elements in wt.%, minor and trace elements in ppm. L – lava, B – bomb, S – scoria. Samples from the Menyailov vents are marked by italics in the "Sample No" column.

Date	27-Nov	27-Nov	27-Nov	27-Nov	27-Nov	27-Nov	27-Nov	28-Nov	28-Nov	2-Dec	2-Dec	2-Dec	2-Dec	7-Dec	7-Dec
Sample No	*Tolb-1201/1 (L)*	*Tolb-1202 (L)*	*Tolb-1203 (L)*	*Tm-08 (L)*	*Tm-09 (L)*	*Tolb-1301 (L)*	*Tolb-1302 (B)*	*Tolb-2808-1 (L)*	*Tolb-2808-2 (L)*	Tm-1 (L)	Tm-2 (L)	Tm-3 (L)	Tm-5 (L)	Tolb-1318 (B)	Tolb-2808-3 (B)
SiO_2	53.76	54.02	54.07	54.68	54.52	53.64	54.46	53.18	53.39	52.41	52.22	52.23	52.53	51.50	51.58
TiO_2	1.82	1.76	1.77	1.70	1.70	1.79	1.71	1.81	1.79	2.00	1.98	1.99	2.02	1.92	1.89
Al_2O_3	16.32	16.42	16.48	16.50	16.52	16.30	16.38	16.26	16.18	15.76	15.78	15.79	15.59	15.37	16.47
FeO	9.20	9.07	8.98	8.65	8.67	9.35	8.81	9.47	9.30	10.32	10.36	10.31	10.26	11.36	10.26
MnO	0.17	0.16	0.16	0.17	0.16	0.16	0.16	0.17	0.17	0.17	0.17	0.17	0.17	0.17	0.17
MgO	3.37	3.29	3.29	2.98	3.06	3.32	3.03	3.45	3.57	3.81	3.87	3.76	3.73	4.36	3.85
CaO	7.26	7.16	7.14	6.67	6.82	7.18	6.80	7.42	7.38	7.56	7.55	7.51	7.50	7.46	7.64
Na_2O	3.81	3.88	3.84	4.04	3.94	3.81	4.02	3.78	3.77	3.52	3.65	3.69	3.72	3.36	3.72
K_2O	2.45	2.47	2.54	2.64	2.54	2.46	2.65	2.44	2.46	2.48	2.44	2.47	2.46	2.31	2.34
P_2O_5	0.69	0.69	0.69	0.77	0.72	0.69	0.75	0.71	0.71	0.60	0.63	0.70	0.68	0.66	0.68
Total	98.84	98.84	98.88	98.79	98.75	98.70	98.77	98.69	98.72	98.63	98.65	98.62	98.66	98.47	98.60
V	264	267	244	214	231	289	228	275	270	260	279	264	269	292	303
Cr	11	17	16	8	13	8	15	9	7	20	23	22	12	34	32
Co	29	25	17	24	23	24	23	26	24	20	26	21	29	40	36
Ni	15	13	12	11	12	17	11	18	15	30	36	32	34	41	36
Zn	106	105	103	112	110	113	114	110	109	108	113	110	106	121	119
Rb	64	63	65	65	65	66	69	68	66	62	66	64	67	64	66
Sr	312	312	310	322	329	320	330	324	327	312	296	295	304	322	323
Y	52	51	48	50	50	49	50	47	48	39	43	42	39	48	47
Zr	257	253	245	262	256	249	269	266	272	227	240	236	236	258	268
Nb	9	9	10	9	8	8	7	9	7	8	10	11	11	8	8
Ba	571	599	592	604	593	591	649	568	559	557	559	581	514	499	561
Pb	5	10	10	<10	<10	<10	<10			11	<10	<10	<10		
Cu	357	334	316	231	256	340	233	358	295	366	381	374	385	374	356

10-Dec	22-Dec	24-Dec	31-Dec	15-Jan	15-Jan	21-Jan	21-Jan	23-Jan	23-Jan	25-Jan	25-Jan	31-Jan	31-Jan	1-Feb
Tm-6 (L)	Tm-10 (L)	7630-03 (L)	Tolb-1204 (S)	Tm-11 (L)	Tm-12 (L)	Tm-13 (L)	Tm-14 (L)	Tolb-1303 (L)	To-01 (L)	Tolb-1304 (L)	To-03 (L)	To-04 (L)	To-05 (L)	To-09 (L)
52.06	51.74	51.83	50.45	51.80	51.90	51.91	51.75	51.79	51.48	51.88	51.60	51.34	51.54	51.41
2.00	1.92	1.95	1.87	1.96	1.93	1.94	1.96	1.93	1.89	1.96	1.91	1.96	1.97	1.96
15.74	16.07	16.11	15.63	16.21	16.19	16.18	16.20	16.19	16.48	16.15	16.39	15.64	15.65	15.78
10.51	10.56	10.38	12.57	10.44	10.39	10.49	10.49	10.46	10.31	10.42	10.41	10.86	10.68	10.68
0.17	0.17	0.16	0.18	0.17	0.17	0.17	0.17	0.17	0.17	0.17	0.17	0.17	0.17	0.17
4.02	4.10	4.11	4.18	4.11	4.08	4.10	4.13	4.10	3.89	4.13	3.97	4.34	4.33	4.21
7.48	7.37	7.32	7.02	7.32	7.35	7.27	7.32	7.33	7.67	7.32	7.61	7.25	7.24	7.29
3.56	3.58	3.64	3.48	3.61	3.61	3.56	3.61	3.62	3.68	3.60	3.51	3.43	3.39	3.49
2.41	2.37	2.38	2.31	2.39	2.38	2.40	2.38	2.39	2.33	2.37	2.34	2.30	2.33	2.33
0.66	0.70	0.71	0.68	0.71	0.70	0.70	0.70	0.71	0.68	0.70	0.67	0.69	0.70	0.68
98.61	98.59	98.60	98.37	98.72	98.70	98.72	98.71	98.70	98.58	98.70	98.58	97.98	98.00	98.00
306	302	296	286	287	271	285	286	281	301	309	291	292	290	290
20	30	25	79	30	25	29	33	44	33	31	27	51	31	36
27	31	31	41	24	31	33	33	25	32	39	25	34	33	35
40	36	38	71	35	36	44	32	42	37	38	36	39	38	40
113	122	118	137	115	106	114	109	113	119	128	116	116	115	118
64	60	60	56	62	61	62	62	61	63	62	68	67	64	66
307	311	311	274	308	305	308	304	301	329	318	325	328	327	329
43	48	49	44	49	47	46	50	51	48	54	45	47	48	46
245	252	245	226	260	250	258	252	243	266	272	266	226	228	228
11	8.1	9	8.1	9	9	11	8.0	8	8	7	8	9	8	9
553	566	588	504	587	566	546	554	526	528	589	520	516	517	498
<10	<10	10	<10	6	6	9	10	9		10		10	5	13
382	360	356	386	356	337	348	338	360	359	389	363	367	356	361
3-Feb	7-Feb	7-Feb	7-Feb	8-Feb	8-Feb	9-Feb	9-Feb	13-Feb	14-Feb	16-Feb	20-Feb	22-Feb	25-Feb	25-Feb

To-10 (L)	To-12 (L)	To-13 (L)	To-16 (L)	To-14 (L)	To-18 (L)	To-17 (L)	To-19 (L)	To-21 (L)	To-23 (L)	D-1304 (L)	D-1306 (L)	D-1307 (L)	D-1309 (L)	D-1310 (L)
51.57	51.90	51.94	51.48	51.71	51.47	51.18	51.79	51.70	51.47	51.45	51.61	51.34	51.41	51.68
1.94	1.90	1.81	1.93	1.95	1.92	1.93	1.89	1.94	1.92	1.93	2.10	1.93	1.95	1.93
16.21	16.15	16.97	15.99	16.02	15.99	16.12	16.71	16.04	16.01	15.84	15.58	15.88	16.17	16.07
10.58	10.35	9.74	10.50	10.60	10.38	10.69	10.12	10.55	10.46	10.75	10.98	10.63	10.67	10.58
0.17	0.17	0.16	0.17	0.17	0.17	0.18	0.17	0.17	0.17	0.17	0.18	0.17	0.18	0.17
4.04	3.89	3.50	4.05	3.95	4.24	4.17	3.55	4.00	4.15	4.11	4.35	4.25	4.04	3.90
7.58	7.28	7.64	7.28	7.23	7.27	7.67	7.53	7.31	7.28	7.23	7.61	7.23	7.56	7.32
3.42	3.66	3.85	3.57	3.65	3.61	3.59	3.77	3.61	3.58	3.47	3.23	3.57	3.49	3.68
2.34	2.36	2.35	2.33	2.35	2.30	2.34	2.37	2.34	2.30	2.33	2.30	2.30	2.37	2.33
0.70	0.73	0.70	0.70	0.73	0.68	0.68	0.71	0.72	0.69	0.68	0.57	0.69	0.70	0.70
98.55	98.38	98.66	98.00	98.33	98.03	98.55	98.61	98.35	98.02	97.97	98.51	97.99	98.54	98.35
287	282	295	298	286	292	286	301	285	292	275	293	300	285	292
37	35	23	40	50	36	43	20	34	22	39	34	19	32	41
28	29	29	27	37	28	30	28	30	33	33	33	32	34	33
38	37	36	37	43	36	38	38	45	35	53	39	86	36	54
116	110	114	115	114	117	118	116	115	118	113	117	119	117	114
63	66	62	63	67	67	65	64	62	63	64	65	67	62	63
326	330	327	329	325	327	325	324	329	328	327	323	326	325	330
47	46	45	48	47	48	46	46	47	48	46	49	46	48	46
261	239	259	234	228	236	266	266	235	235	228	271	230	264	234
9	8	8	9	9	9	8	8	7	9	8	8	8	8	9
514	542	559	549	521	530	485	544	547	541	531	527	521	529	534
	<5		<5	<5	<5			<5	6	<5		6		<5
358	367	353	357	352	357	358	348	407	361	407	363	504	364	405
28-Feb	4-Mar	4-Mar	5-Mar	5-Mar	8-Mar	19-Mar	25-Mar	1-Apr	1-Apr	2-Apr	4-Apr	5-Apr	8-Apr	13-Apr

D-1312 (L)	D-1313 (L)	To-24 (L)	D-1314 (L)	D-1317 (L)	D-1316 (L)	Tl-2013-L3	Tl-2013-L5	To-25 (L)	Tl-2013-L7	Tl-2013-L9	Tl-2013-L13	Tl-2013-L15	Tl-2013-L19	Tolb-1313 (L)
51.23	51.37	51.48	51.71	51.50	51.49	52.10	51.42	51.62	52.05	52.02	51.95	51.87	51.95	51.50
1.93	1.96	1.94	2.05	1.94	1.97	1.93	1.97	1.93	1.91	1.92	1.94	1.91	1.94	1.92
15.80	15.77	16.11	15.76	16.17	15.63	15.89	16.06	15.76	16.08	16.30	15.85	16.03	16.02	16.42
10.74	10.51	10.61	10.79	10.50	10.70	10.73	10.68	10.60	10.57	10.55	10.81	10.61	10.77	10.36
0.17	0.17	0.18	0.17	0.18	0.17	0.17	0.18	0.17	0.17	0.17	0.17	0.17	0.17	0.17
4.35	4.48	4.11	4.35	4.17	4.32	4.26	4.10	4.24	4.17	3.91	4.33	4.42	4.11	4.06
7.25	7.26	7.63	7.62	7.64	7.23	6.95	7.57	7.21	7.01	6.98	6.99	6.95	6.99	7.60
3.54	3.52	3.49	3.24	3.46	3.45	3.40	3.50	3.44	3.49	3.62	3.37	3.53	3.48	3.55
2.29	2.29	2.33	2.27	2.32	2.33	2.35	2.37	2.32	2.34	2.34	2.36	2.32	2.35	2.34
0.68	0.69	0.69	0.56	0.69	0.70	0.71	0.70	0.70	0.71	0.70	0.70	0.70	0.71	0.67
97.98	98.02	98.56	98.52	98.57	97.99	98.49	98.55	97.99	98.50	98.51	98.47	98.51	98.49	98.59
297	292	298	294	298	288	285	291	292	289	280	285	287	295	297
26	33	30	24	32	44	35	28	32	33	38	35	28	31	33
27	34	30	30	30	32	35	25	31	30	27	32	30	30	34
41	40	35	38	40	37	40	37	38	36	38	43	37	39	36
116	120	117	120	118	117	114	116	118	117	114	115	117	114	119
67	65	63	64	66	61	68	62	64	64	63	61	65	65	66
327	328	324	325	324	327	326	326	328	326	325	325	326	325	325
48	49	49	49	48	49	47	46	46	48	48	50	49	47	48
228	232	263	264	265	228	264	269	231	268	260	266	262	263	265
8	8	8	8	8	9	8	8	8	7	8	8	8	8	8
560	545	503	530	519	523	521	503	545	561	513	522	506	478	535
<5	6				<5			5						
370	365	361	363	355	362	350	364	367	364	357	362	360	356	364
20-Apr	26-Apr	23-May	28-May	28-May	17-Jul	18-Jul	19-Jul	20-Jul	21-Jul	24-Jul	15-Aug	16-Aug	29-Aug	29-Aug

Tolb-1314 (L)	Tolb-1315 (L)	Tl-2013-B13	Tl-2013-L36	Tl-2013-L37	Tl-2013-L41	Tl-2013-L44	Tl-2013-B17	Tl-2013-L45	Tl-2013-B22	Tl-2013-L47	Tolb-1316 (B)	Tolb-1317-2 (L)	Tolb-2908-1 (B)	Tolb-2908-2 (B)
52.12	51.18	51.44	51.37	51.62	51.54	51.53	51.53	51.75	51.84	50.68	51.58	51.64	51.65	51.70
1.93	1.95	1.92	1.95	1.92	1.89	1.95	1.94	1.88	1.88	1.93	1.90	1.88	1.89	1.87
16.21	16.04	16.13	16.15	16.36	16.65	16.15	16.04	16.22	16.98	15.95	16.25	16.41	16.29	16.34
10.54	11.09	10.58	10.64	10.27	10.28	10.56	10.64	10.34	9.90	10.63	10.32	10.17	10.28	10.25
0.17	0.18	0.18	0.17	0.17	0.17	0.17	0.17	0.17	0.17	0.18	0.17	0.17	0.17	0.17
4.12	4.10	4.16	4.13	4.12	3.79	4.09	4.13	4.22	3.27	4.22	4.17	4.13	4.15	4.17
6.90	7.52	7.62	7.57	7.53	7.65	7.59	7.58	7.63	7.67	7.82	7.59	7.57	7.55	7.56
3.48	3.42	3.51	3.51	3.54	3.57	3.48	3.45	3.40	3.87	3.99	3.59	3.58	3.57	3.53
2.35	2.33	2.34	2.35	2.36	2.36	2.35	2.37	2.30	2.39	2.48	2.33	2.37	2.35	2.32
0.70	0.69	0.68	0.69	0.71	0.68	0.69	0.70	0.67	0.69	0.68	0.69	0.69	0.69	0.69
98.51	98.49	98.56	98.54	98.59	98.59	98.56	98.55	98.58	98.65	98.56	98.59	98.61	98.59	98.60
282	289	294	305	293	290	301	301	296	297	278	290	295	293	293
42	57	35	66	45	29	36	42	50	28	38	34	30	60	36
30	36	31	29	31	27	29	33	35	26	33	31	35	34	34
35	44	37	38	40	38	39	40	39	35	37	42	39	43	43
114	119	121	121	115	119	118	121	119	114	116	120	118	121	116
62	63	68	60	67	62	66	65	64	66	67	66	66	65	65
324	322	324	325	326	326	325	325	318	325	323	324	323	326	326
47	50	46	48	46	46	46	48	49	46	48	49	46	46	47
266	265	269	264	269	266	265	265	272	266	265	265	265	266	266
7	8	9	8	8	8	9	8	9	8	8	8	9	8	8
490	544	514	539	540	516	521	550	504	516	502	506	540	540	535
356	360	364	355	371	363	360	354	351	353	349	356	355	363	359

Table 2. Concentrations of trace elements in the rocks of the 2012-2013 Tolbachik fissure eruption (in ppm). Samples analyzed in GZG, Georg-August Universität Göttingen, are marked by bold type in the "Sample No" column; Menyailov vent lava samples are marked by italics. L – lava, B – bomb, S – scoria.

	Tolb 1201 /1 (L)	*Tol b 120 2 (L)*	*Tol b 120 3 (L)*	*Tm 8 (L)*	Tm 1 (L)	Tm 6 (L)	Tm 10 (L)	Tm 14 (L)	Tol b 120 4 (S)	To-17 (L)	D-130 7 (L)	**D-131 4 (L)**	Tl-201 3-L5	**Tol b-131 3 (L)**	Tol b-131 5 (L)	**Tl-201 3-L41**	Tl-201 3-L44	Tl-201 3-B17	Tl-201 3-L45	**Tl-201 3-B22**	**Tl-201 3-L47**	Tol b-131 7-2 (L)	Tol b-290 8-2 (B)
Li	21.69	21.03	20.86	20.87	18.46	17.88	18.18	18.40	19.57	17.90	18.64	20.84	18.46	20.86	18.17	20.91	18.34	18.42	17.99	21.02	20.61	18.20	17.94
Be	2.04	2.07	2.02	2.05	1.87	1.83	1.88	1.92	1.92	2.08	2.15		2.12		2.06		2.09	2.16	2.11			2.11	2.13
Sc	27.31	27.26	26.46	25.82	30.32	29.33	28.27	26.93	27.51	25.21	24.99	27.25	24.80	27.52	24.80	27.82	25.07	24.83	24.68	28.09	27.89	24.65	24.50
Co	25.91	25.79	25.98	23.61	31.56	32.71	34.65	35.02	38.27	33.35	33.75	32.42	32.56	32.59	32.99	32.98	33.12	32.94	32.78	32.81	33.27	32.57	32.84
Ni	11.11	10.03	8.16	5.91	18.39	25.69	29.46	30.00	62.42	41.51	81.71	37.66	38.61	37.84	43.53	38.65	41.14	39.92	39.46	36.56	39.28	39.04	38.52
Cu	325	295	284	185	290	270	289	299	327	315	445	214	323	214	322	214	308	317	313	215	218	305	294
Zn	149	125	120	108	109	106	121	118	138	118	122	128	122	129	123	129	126	131	129	130	132	126	119
Ga	19.83	19.62	20.83	21.33	21.07	21.09	20.89	20.46	21.05	20.43	20.10	20.97	20.20	21.24	20.06	20.94	19.89	20.04	20.15	21.17	21.16	19.82	19.92
Y	47.70	47.36	48.92	49.15	45.54	45.85	45.97	44.69	44.69	42.42	41.96	42.81	42.31	43.16	42.11	42.83	42.58	43.13	42.05	43.67	43.09	41.86	42.23
Zr	295	291	301	308	277	282	283	276	275	311	308	278	310	278	307	280	310	312	311	283	282	306	309
Nb	8.98	8.60	8.87	8.88	8.09	8.10	8.11	8.01	8.11	7.59	7.50	7.52	7.30	7.59	7.29	7.53	7.43	7.80	7.41	7.63	7.49	7.21	7.27
Rb	79.97	79.14	83.92	92.10	81.16	80.96	80.04	78.20	83.55	71.96	72.00	68.54	71.85	68.35	72.36	68.16	73.22	73.37	72.89	68.45	68.35	72.25	72.90
Sr	345	352	360	377	351	348	361	357	359	326	327	328	330	327	329	329	332	334	332	326	330	329	321
Cs	2.34	2.30	2.43	2.66	2.37	2.26	2.26	2.22	2.31	2.24	2.26	2.18	2.24	2.21	2.21	2.18	2.31	2.26	2.23	2.19	2.14	2.24	2.24
Ba	640	645	652	705	619	596	619	614	617	580	594	566	588	565	575	562	570	576	569	563	566	559	550
	22.3	22.0	22.9	23.7	21.6	21.5	21.2	20.6	21.1	21.9	21.7	22.9	21.7	22.9	21.6	22.8	21.9	22.0	21.8	22.9	23.0	21.4	21.4

La	2	1	6	1	6	0	2	2	7	1	9	1	8	3	2	6	3	3	7	8	3	7	9
Ce	56.51	55.61	57.89	63.64	57.71	54.95	55.25	54.18	54.34	54.52	54.40	55.21	54.02	55.08	54.08	54.90	54.91	55.11	54.67	55.05	55.13	53.71	54.00
Pr	7.81	7.55	7.88	8.19	7.60	7.56	7.44	7.30	7.48	7.88	7.64	8.19	7.69	8.23	7.65	8.22	7.76	7.76	7.73	8.24	8.26	7.58	7.78
Nd	35.74	34.44	35.77	37.70	34.43	34.76	34.51	33.80	33.73	35.02	35.06	37.47	34.59	37.54	34.59	37.34	35.11	35.18	34.89	37.51	37.58	34.43	34.55
Sm	8.36	8.24	8.54	9.03	8.28	8.41	8.24	8.22	8.13	8.45	8.42	8.83	8.39	8.81	8.35	8.73	8.36	8.49	8.43	8.71	8.67	8.38	8.37
Eu	2.22	2.15	2.25	2.35	2.15	2.22	2.18	2.10	2.07	2.22	2.21	2.41	2.19	2.39	2.17	2.41	2.19	2.21	2.22	2.41	2.37	2.19	2.20
Gd	8.60	8.49	8.69	8.96	8.14	8.30	8.19	8.17	8.14	8.65	8.58	7.74	8.54	7.74	8.48	7.82	8.44	8.67	8.58	7.85	7.81	8.47	8.50
Tb	1.30	1.27	1.34	1.37	1.25	1.26	1.20	1.22	1.24	1.33	1.33	1.35	1.31	1.34	1.32	1.35	1.29	1.34	1.33	1.34	1.35	1.32	1.31
Dy	7.78	7.59	8.02	7.92	7.34	7.41	7.34	7.25	7.25	7.70	7.69	7.94	7.59	8.02	7.57	7.95	7.70	7.69	7.73	7.95	7.94	7.55	7.65
Ho	1.56	1.53	1.59	1.65	1.53	1.53	1.53	1.51	1.51	1.53	1.55	1.64	1.54	1.64	1.53	1.63	1.57	1.55	1.53	1.64	1.62	1.55	1.55
Er	4.64	4.56	4.75	4.83	4.49	4.46	4.54	4.39	4.39	4.51	4.56	4.61	4.47	4.57	4.51	4.54	4.54	4.54	4.51	4.58	4.56	4.50	4.50
Tm	0.65	0.65	0.67	0.69	0.63	0.63	0.63	0.61	0.62	0.63	0.64	0.64	0.64	0.65	0.62	0.65	0.64	0.64	0.64	0.65	0.65	0.64	0.63
Yb	4.36	4.20	4.43	4.51	4.09	4.08	4.06	4.00	3.98	4.29	4.18	4.39	4.19	4.39	4.18	4.40	4.27	4.27	4.20	4.42	4.36	4.22	4.23
Lu	0.66	0.64	0.68	0.69	0.63	0.61	0.63	0.60	0.62	0.64	0.63	0.63	0.64	0.64	0.63	0.63	0.64	0.65	0.64	0.63	0.62	0.63	0.64
Hf	7.27	7.02	7.27	7.31	6.67	6.68	6.66	6.45	6.43	6.76	6.73	6.83	6.65	6.85	6.71	6.82	6.78	6.77	6.75	6.95	6.88	6.73	6.73
Ta	0.63	0.59	0.60	0.54	0.55	0.51	0.51	0.48	0.46	0.69	0.71	0.45	0.68	0.46	0.55	0.45	0.69	0.58	0.67	0.46	0.46	0.65	0.57
Tl	0.10	0.11	0.12	0.12	0.09	0.07	0.07	0.08	0.10	0.09	0.08	0.08	0.07	0.08	0.07	0.08	0.07	0.10	0.10	0.07	0.07	0.07	0.07
Pb	8.44	8.18	8.19	9.67	8.39	8.36	8.25	7.86	8.18	7.43	7.78	6.38	7.51	6.39	7.46	6.25	7.50	8.04	8.02	6.38	6.31	7.31	7.51
Th	3.67	3.51	3.69	3.18	2.72	2.76	2.74	2.67	2.87	2.88	2.77	2.87	2.76	2.86	2.79	2.82	2.83	3.32	2.86	2.88	2.84	2.79	2.78
U	1.82	1.78	1.88	2.27	1.97	1.97	1.94	1.92	2.00	1.64	1.64	1.66	1.64	1.66	1.66	1.64	1.68	1.72	1.67	1.68	1.66	1.64	1.68